

Highlights

- H₂ supersaturates in the liquid phase at 100 rpm despite hyperthermophilic conditions.
- High H_{2aq} concentrations directly inhibit the specific rates of dark fermentation.
- H₂ supersaturation and H₂ production rate depend on the gas-liquid mass transfer.
- H₂-rich biogas recirculation is an effective method to prevent H₂ supersaturation.
- Gas recirculation increased the hydrogen production rate by 271%.

1 **H₂-rich biogas recirculation prevents hydrogen supersaturation and enhances**
2 **hydrogen production by *Thermotoga neapolitana* cf. *capnolactica***

3 Gilbert Dreschke^{a, b, *}, Stefano Papirio^c, Giuliana d'Ippolito^b, Antonio Panico^d, Piet N.L. Lens^e,

4 Giovanni Esposito^a, Angelo Fontana^b

5

6 ^aDepartment of Civil and Mechanical Engineering, University of Cassino and Southern Lazio,

7 Via Di Biasio, 43, 03043 Cassino, FR, Italy. (E-mail: giovanni.esposito@unicas.it)

8 ^bBio-Organic Chemistry Unit, Institute of Biomolecular Chemistry, Italian National Council of

9 Research, Via Campi Flegrei 34, 80078 Pozzuoli, NA, Italy. (E-mails: gdippolito@icb.cnr.it,

10 afontana@icb.cnr.it)

11 ^cDepartment of Civil, Architectural and Environmental Engineering, University of Napoli

12 Federico II, Via Claudio 21, 80125 Napoli, Italy. (stefano.papirio@unina.it)

13 ^dTelematic University Pegaso, Piazza Trieste e Trento, 48, 80132, Napoli, Italy. (E-mail:

14 antonio.panico@unipegaso.it)

15 ^eUNESCO - IHE Institute for Water Education, Westvest 7, 2611-AX Delft, The Netherlands.

16 (E-mail: p.lens@unesco-ihe.org)

17

18

19 * Corresponding author

20 Gilbert Dreschke MSc

21 Present address:

22 Department of Civil and Mechanical Engineering, University of Cassino and Southern Lazio,

23 Via Di Biasio 43, 03043 Cassino, FR, Italy

24 Email: g.dreschke@unicas.it

25 **Abstract**

26 This study focused on the supersaturation of hydrogen in the liquid phase (H_{2aq}) and its
27 inhibitory effect on dark fermentation by *Thermotoga neapolitana* cf. *capnolactica* by
28 increasing the agitation (from 100 to 500 rpm) and recirculating H_2 -rich biogas (GaR). At low
29 cell concentrations, both 500 rpm and GaR reduced the H_{2aq} from 30.1 (\pm 4.4) mL/L to the
30 lowest values of 7.4 (\pm 0.7) mL/L and 7.2 (\pm 1.2) mL/L, respectively. However, at high cell
31 concentrations (0.79 g CDW/L), the addition of GaR at 300 rpm was more efficient and
32 increased the hydrogen production rate by 271%, compared to a 136% increase when raising
33 the agitation to 500 rpm instead. While H_{2aq} primarily affected the dark fermentation rate,
34 GaR concomitantly increased the hydrogen yield up to 3.5 mol H_2 /mol glucose. Hence, H_{2aq}
35 supersaturation highly depends on the systems gas-liquid mass transfer and strongly inhibits
36 dark fermentation.

37

38

39

40

41

42

43

44

45 **Key words:** *Thermotoga neapolitana*; Dark fermentation; Gas recirculation; Sparging;
46 Hydrogen supersaturation; End product inhibition

47

48 Declarations of interest: none

49 **Highlights**

- 50 • H₂ supersaturates in the liquid phase at 100 rpm despite hyperthermophilic
51 conditions.
- 52 • High H_{2aq} concentrations directly inhibit the specific rates of dark fermentation.
- 53 • H₂ supersaturation and H₂ production rate depend on the gas-liquid mass transfer.
- 54 • H₂-rich biogas recirculation is an effective method to prevent H₂ supersaturation.
- 55 • Gas recirculation increased the hydrogen production rate by 271%.

56

57

58

59

60 **Abbreviations**

61 AA acetic acid

62 BGR biomass growth rate

63 BMY biomass yield

64 CSTR continuously stirred tank reactor

65 GaR recirculation of H₂-rich biogas

66 GCR glucose consumption rate

67 H_{2aq} liquid phase hydrogen

68 HPR hydrogen production rate

69 HY hydrogen yield

70 LA lactic acid

71 1. Introduction

72 Hydrogen, a nonpolluting energy carrier can be produced from organic residues in an
73 environmental-friendly biological process called dark fermentation [1,2]. Hydrogen
74 production has been reported in a wide range of temperatures, with thermophilic conditions
75 being generally correlated to higher hydrogen yields (HY) [1,2]. A variety of microbial species
76 are capable of fermentative hydrogen production [3] in both mixed and pure culture
77 applications [4]. The use of mixed cultures is considered to be the simpler and have a more
78 practical approach [4], but often entailing the coexistence of microorganisms which do not
79 produce or even consume hydrogen [5].

80 *Thermotoga neapolitana* (hereafter *T. neapolitana*) is a hyperthermophilic microorganism
81 with a high potential for hydrogen production via dark fermentation [6,7]. Some of the key
82 characteristics exhibited by this organism include fast growth kinetics [7], and efficient
83 degradation of a wide range of substrates, e.g. glucose, fructose, xylose, maltose, starch
84 [7,8], molasses, cheese whey [9], algal biomass [10], and carrot pulp [11]. *T. neapolitana* is
85 capable to approach the theoretical HY of 4 mol H₂/mol glucose by optimizing the conditions
86 for the hydrogen forming acetate pathway [12,13]. Additionally, the hyperthermophilic
87 culture conditions of *T. neapolitana* further stimulate the reaction rates [2] and hamper the
88 growth competitive microorganisms [14], also leading to a pasteurization of the used
89 substrate [15].

90 In dark fermentative hydrogen production, the presence of hydrogen is one of the most
91 crucial factors, as high concentrations of hydrogen are a major inhibitor of the process. To
92 reduce the inhibitory effect of hydrogen on the process, previous experimental studies
93 (Table 1) have employed a variety of techniques, e.g. sparging the headspace, reducing the
94 total pressure, applying vigorous stirring, optimizing the reactor design, or simply increasing

95 the headspace/solution ratio [12]. Regardless of the method used, alleviation of hydrogen
96 inhibition results in increased HYs and/or hydrogen production rates (HPR).
97 The headspace hydrogen concentration has been widely used (Table 1) to predict hydrogen
98 in the liquid phase (H_{2aq}), which *de facto* acts on the microbial cultures. However, poorly
99 soluble gases, such as hydrogen, supersaturate in solution during anaerobic processes
100 [31,32]. Studies, including a direct measurement of H_{2aq} (Table 1), have observed that H_{2aq}
101 can exceed the equilibrium concentration suggested by Henry's law multiple times. As a
102 result, the measurement of headspace hydrogen is considered inappropriate to predict the
103 H_{2aq} value [2,16–18,31,32].

104 Our study focused on the effect of agitation and biogas recirculation on the accumulation of
105 H_{2aq} and the consequent impact on dark fermentation by *T. neapolitana*. The main goal was
106 to demonstrate that the recirculation of the H_2 -rich biogas (GaR) into the culture broth is an
107 effective method to improve the gas-liquid mass transfer and prevent H_{2aq} from
108 supersaturating, without diluting the H_2 percentage in the biogas. Furthermore, we wanted
109 to show that keeping the H_{2aq} in equilibrium with the gas phase is sufficient to achieve high
110 hydrogen production yields and rates. In a first assay, the effect of GaR and agitation speed
111 on hydrogen production was evaluated using a highly concentrated *T. neapolitana* culture. In
112 a second assay, a direct measurement of H_{2aq} was included to demonstrate the correlation
113 between hydrogen supersaturation and the performance of dark fermentation.

114

115 **2. Material and methods**

116 **2.1. Bacterial culture and medium**

117 A pure culture of *Thermotoga neapolitana cf. capnolactica* [33] was used in all experiments.
118 The cultivation and storage conditions for the culture, the preparation of inoculum for
119 elevated cell concentrations (assay 1) and the modified ATCC 1977 medium used (containing
120 27.8 mM of glucose) were as described by Dreschke et al. [34]. The pH of the medium was
121 adjusted to 7.5 prior to being autoclaved at 110 °C for 5 min. Prior to the inoculation, the
122 medium was heated at 80 °C for 30 min and sparged with N₂ for 5 min to remove the
123 dissolved oxygen.

124 **2.2. Experimental design**

125 All experiments were run in a 3-L fully controlled continuously stirred tank reactor (CSTR)
126 (Applikon Biotechnology, the Netherlands) with a working volume of 2 L. The operating
127 temperature was kept at a constant 80 °C and pH was automatically adjusted to 7 by adding
128 1M NaOH. GaR was applied by continuously pumping the produced biogas from the
129 headspace to a gas dispersion device at the base of the reactor at a flow rate of 350 mL/min.
130 The produced biogas was released into 500 mL water displacement systems to avoid
131 pressure build-up and quantified every hour. Liquid samples of 2 mL were withdrawn each
132 30 or 60 min. The fermentation was considered completed when the reactors ceased to
133 produce biogas. Fermentation time was approximated from the inoculation to the end of the
134 fermentation. Each condition was conducted in duplicate to demonstrate reproducibility.

135 **2.2.1. Assay 1 – Effect of agitation speed and gas recirculation on dark** 136 **fermentation at high cell concentrations**

137 Assay 1 was designed to study the effect of GaR and agitation speed on the dark
138 fermentation process at high cell concentrations of *T. neapolitana*. The reactor was
139 inoculated with 80 mL of concentrated inoculum [34] resulting in a biomass concentration of
140 0.79 (\pm 0.03) g cell dry weight (CDW)/L. The following operating conditions were
141 investigated: 300 rpm agitation (300); 300 rpm agitation with gas recirculation (300 + GaR);
142 500 rpm agitation (500); 500 rpm agitation with gas recirculation (500 + GaR).

143 **2.2.2. Assay 2 – Effect of GaR and agitation speed on H_{2aq}**

144 Assays 2A and 2B were designed to study the effect of agitation speed and GaR on the
145 retention of hydrogen in the liquid phase and its influence on the dark fermentation process.
146 The reactor was inoculated with 20 mL of storage culture (1% v/v) and maintained for 15 h
147 at 100 rpm to acclimatize the culture. Afterwards, a sequence of operating conditions was
148 used with each condition being operated for 2 h as described in Table 2. In assay 2A, 5 min of
149 500 rpm + GaR (Table 2 – shaded grey cells) was used before each operating condition to
150 remove the accumulated hydrogen from the liquid phase. After 5 or 30 min and at the end
151 of each operating condition, 20 mL of broth was withdrawn to monitor H_{2aq}.

152 **2.3. Analytical Methods**

153 **2.3.1. Assay 1**

154 Cell growth was determined by measuring spectrophotometrically (Lambda 365, Perkin
155 Elmer, USA) optical density (OD₅₄₀) of the liquid samples at 540 nm. Liquid samples were
156 centrifuged at 10,000 rpm for 5 min to collect the supernatant for the determination of
157 glucose, acetic acid (AA), lactic acid (LA) and alanine concentration as described by Dreschke
158 et al. [34]. The glucose concentration was measured by the dinitrosalicylic acid method [35],
159 while AA, LA and alanine were quantified by ¹H Nuclear Magnetic Resonance (NMR) with a

160 600 MHz spectrometer (Bruker Avance 400) as described by Dipasquale et al. [10]. After the
161 completion of the fermentation, 500 mL of culture broth was centrifuged at 3750 rpm for 20
162 min for the determination of CDW via freeze drying. The concentration of hydrogen in the
163 produced gas was analyzed by gas chromatography as described by Dipasquale et al. [10].
164 The conversion from volumetric to molar H₂ production was performed using the ideal gas
165 law.

166 **2.3.2. Assay 2**

167 Glucose, AA and LA concentrations were determined using an HPLC (Prominence LC-20A
168 Series, Shimadzu, Japan), equipped with UV/Vis (SPD-20A, Shimadzu Japan) and refractive
169 index (RID-20A, Shimadzu, Japan) detectors, with the method described by Mancini et al.
170 [36] with 0.0065 M of sulfuric acid as the mobile phase. The concentration of hydrogen in
171 the biogas was determined with a Varian 3400 gas chromatograph (GC), equipped with a
172 thermal conductivity detector (TCD) and a Restek packed column using argon as the carrier
173 gas.

174 For the determination of H_{2aq}, a modified method of Kraemer and Bagley [16,17,37] was
175 applied. Vials with a total volume of 31 mL were closed with silicon septa and depressurized
176 using a plastic syringe. 20 mL of sample was injected into the vials and immediately placed
177 upside down in fridge to equilibrate the liquid and the gas phases. After around 20 h, the
178 sample was heated at room temperature and the negative pressure equilibrated by adding
179 air to the gas phase of the sample. The concentration of hydrogen in the gas phase was
180 measured by the GC described above and referred to the 20 mL of liquid sample.

181 **2.4. Kinetic study of dark fermentation**

182 The rates and lag phases of dark fermentation were evaluated in terms of biomass growth,
183 hydrogen production and glucose consumption and calculated by fitting the experimental
184 data with a modified Gompertz model as described by Dreschke et al. [34].

185 **2.5. Statistical analysis**

186 The statistical significance of the experimental data was determined by the calculation of the
187 p-value applying an unpaired t-test with Microsoft Excel 2016 (Microsoft Corporation, USA).

188 **3. Results**

189 **3.1. Effect of agitation speed and GaR on dark fermentation at high cell concentrations** 190 **(assay 1)**

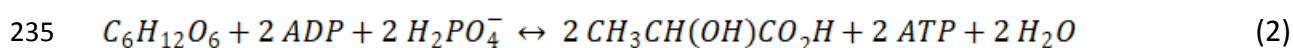
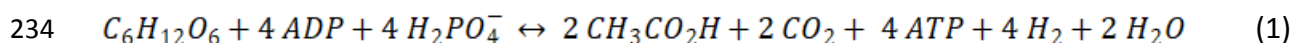
191 Fig. 1. shows the glucose consumption (A), cumulative hydrogen (B) and biomass growth (C)
192 during batch fermentation with an initial cell concentration of $0.79 (\pm 0.03)$ g CDW/L of *T.*
193 *neapolitana* using an agitation of 300 or 500 rpm with and without GaR.
194 Increasing the agitation significantly enhanced the specific rates of biomass growth [mg
195 CDW/h/g CDW], hydrogen production [mL H₂/h/g CDW], and glucose consumption [mmol
196 glucose/h/g CDW] from $73 (\pm 11)$, $294 (\pm 44)$, and $4.4 (\pm 1.3)$ at 300 rpm to $266 (\pm 9)$ (p-value:
197 0.003), $695 (\pm 46)$ (p-value: 0.012), and $10.1 (\pm 0.6)$ (p-value: 0.028) at 500 rpm (Fig. 2, Table
198 3), respectively. Due to the accelerated process, the fermentation time and lag phase of
199 hydrogen production were reduced from 11 h and $2.9 (\pm 0.2)$ h at 300 rpm to 6 h and from
200 $1.3 (\pm 0.1)$ h at 500 rpm (Table 3), respectively. The HY increased from $3.0 (\pm 0.0)$ at 300 rpm
201 to $3.2 (\pm 0.1)$ mol H₂/mol glucose at 500 rpm, while the biomass yield (BMY) increased from
202 approximately 16.7 to 21.9 g CDW/mol glucose (Table 4). The composition of the end
203 products, expressed in terms of an LA/AA ratio, decreased from 0.31 at 300 rpm to 0.21 at
204 500 rpm (Table 5).

205 A combination of GaR and agitation speed at 300 rpm further accelerated the dark
206 fermentation. The specific biomass growth rate reached $423 (\pm 9)$ mg CDW/h/g CDW (p-
207 value: 0.004), while the specific rates of hydrogen production and glucose consumption
208 increased up to $1090 (\pm 91)$ mL/h/g CDW (p-value: 0.032) and $13.3 (\pm 0.8)$ mmol glucose/h/g
209 CDW (p-value: 0.040), respectively, over those obtained at 500 rpm without GaR (Fig. 2,
210 Table 3). The fermentation was completed within 4 h with a lag phase of $0.4 (\pm 0.0)$ h (Table
211 3), a HY of $3.5 (\pm 0.2)$ mol H₂/mol glucose, an approximate BMY of 24.8 g CDW/mol glucose
212 (Table 4), and a LA/AA ratio of 0.11 (Table 5).

213 Increasing the agitation to 500 rpm while applying GaR had no significant effect on the
214 process, as shown by the similar performance obtained at 300 rpm + GaR and 500 rpm + GaR
215 (Fig. 1). At 500 rpm + GaR, the specific rates of biomass growth, hydrogen production and
216 glucose consumption were $431 (\pm 9)$ mg CDW/h/g CDW, $1016 (\pm 22)$ mL H₂/h/g CDW and
217 $12.7 (\pm 0.2)$ mmol glucose/h/g CDW (Fig. 2, Table 3), respectively. The HY reached $3.3 (\pm 0.1)$
218 mol H₂/mol glucose (Table 4) coupled with a LA/AA ratio of 0.13 (Table 5). The fermentation
219 time and lag phase of hydrogen production remained at 4 h and $0.5 (\pm 0.1)$ h (Table 3),
220 respectively, with an approximate BMY of 27.7 g CDW/mol glucose.

221 The highest volumetric HPRs of $850 (\pm 71)$ and $813 (\pm 18)$ mL/h/L were obtained when GaR
222 was applied at 300 and 500 rpm, respectively (Table 3). The hydrogen concentration in the
223 biogas produced was not affected by the use of GaR or the agitation speed and remained
224 constant at $65 (\pm 2)\%$ (data not shown) under all studied conditions. In all bioassays, glucose
225 was consumed up to 82 - 89 % (Table 4) with AA and LA as the main fermentation end
226 products in the digestate and alanine constituting a minor proportion of 2% (Table 5). A
227 mass balance based on the stoichiometric equations 1 and 2 was performed to validate the
228 experimental results. The dark fermentation model suggests the formation of two moles of

229 fermentation end products (AA and LA) per mole of glucose with the concomitant
230 production of 2 moles of hydrogen per mole of AA. Under all operating conditions, the sum
231 of fermentation products in the digestate reached 92% or more of the theoretical value
232 calculated from the glucose consumption and 2.08 (\pm 0.01) moles H₂ per mole of AA were
233 averagely produced.



236

237 **3.2. Effect of GaR and agitation speed on H_{2aq} and HPR (assay 2)**

238 **3.2.1. Assay 2A – Use of different agitation speeds**

239 Assay 2A assessed the effect of the agitation speed on H_{2aq} and HPR. After the initial 15 h at
240 100 rpm, H_{2aq} accumulated up to 30.1 (\pm 4.4) mL/L (Fig. 3B). Then, using 500 rpm + GaR for 5
241 min before each operating condition reduced H_{2aq} to an average of 7.5 (\pm 1.0) mL/L (Fig. 4A).
242 The subsequent agitation of the culture at 300 and 500 rpm without GaR for 2 h led to a H_{2aq}
243 of 17.0 (\pm 2.3) and 7.4 (\pm 0.7) mL/L, respectively (Fig. 3B).

244 To better demonstrate the effect of hydrogen retention in the liquid phase on the HPR, the 2
245 h duration of each operating condition was subdivided in 3 phases and the HPR was
246 calculated for each individual phase: 1 – removal phase, i.e. period from 0 to 5 min after
247 changing the operating condition when additional GaR was applied (“HPR GaR”); 2 –
248 retention phase, i.e. period from 5 to 30 min after changing the operating condition (“HPR
249 post GaR”); 3 – equilibrium phase, i.e. period from 30 to 120 min after changing the
250 operating condition (“HPR”) (Fig. 3A). At 300 rpm, a significantly higher “HPR GaR” of 316 (\pm
251 54) mL/L/h (Fig. 3A) was observed than “HPR” of 54 (\pm 13) mL/L/h (p-value: 0.0002) and

252 “HPR post GaR” of $19 (\pm 17)$ mL/L/h (p-value: 0.0017), respectively. In contrast, at 500 rpm,
253 the HPR remained similar before, during, and after GaR. The “HPR” reached $112 (\pm 22)$
254 mL/L/h, which was not significantly different from “HPR post GaR” ($100 (\pm 16)$ mL/L/h, p-
255 value: 0.397) and “HPR GaR” ($120 (\pm 11)$ mL/L/h, p-value: 0.614) (Fig. 3A). Changing the
256 agitation from 300 to 500 rpm roughly doubled the “HPR”, and concomitantly increased the
257 glucose consumption rate (GCR) from $3.6 (\pm 0.4)$ to $4.7 \pm (0.3)$ mmol/L/h (p-value: 0.016)
258 (data not shown).

259 **3.2.2. Assay 2B – Gas sparging**

260 Assay 2B was run to assess the effect of GaR on H_{2aq} and HPR at a constant agitation at 200
261 rpm. Similar to assay 2A, the highest H_{2aq} of $26.8 (\pm 3.6)$ mL/L (Fig. 4B and C) was obtained
262 after 15 h of operation at 100 rpm. Applying 200 rpm + GaR rapidly decreased the H_{2aq} to 9.0
263 (± 1.8) mL/L in 5 min (Fig. 4B and C) reaching a final value of $7.2 (\pm 1.2)$ mL/L after 2 h (Fig.
264 4B). The 200-rpm agitation without GaR caused an accumulation of H_{2aq} up to a
265 concentration of $16.4 (\pm 0.9)$ mL/L in 30 min, which was 91% of $18.0 (\pm 0.9)$ mL/L reached
266 after 2 h (Fig. 4B and C). The “HPR” at 200 rpm + GaR of $91 (\pm 20)$ mL/L/h was significantly
267 higher than $47 (\pm 8)$ mL/L/h (p-value: 0.017) obtained at 200 rpm without GaR (Fig. 3A).
268 Concomitantly, the GCR reached values of $4.2 (\pm 0.1)$ and $3.1 (\pm 0.8)$ mmol/L/h (p-value:
269 0.077), at 200 rpm + GaR and 200 rpm without GaR, respectively (data of GCR not shown).
270 When agitation was increased from 100 to 200 rpm after 15 h in the absence of GaR, H_{2aq}
271 decreased from 29.4 to 24.8 mL/L in 2 h (Fig. 4C), which was higher than $18.7 (\pm 4.6)$ mL/L
272 obtained at 200 rpm agitation at 21 h after applying GaR between 17 and 19 h.

273 **4. Discussion**

274 **4.1. Effect of agitation speed and gas recirculation on H_{2aq} concentration**

275 In this study, GaR and agitation speed were examined as strategies to lower H_{2aq} and, thus,
 276 stimulate H_2 production by *T. neapolitana*. Agitating at 100 rpm led to the highest H_{2aq} ,
 277 i.e. 30.1 (\pm 4.4) mL/L, which was approximately 3 times higher than the theoretical dissolved
 278 hydrogen concentration (i.e. 9.7 mL/L) in equilibrium with a gas phase containing 65% H_2 at
 279 80 °C according to Henry's Law (Eq. 3):

$$280 \quad H(T) = H^\theta * \exp\left(\frac{d \ln(H)}{d(1/T)} * \left(\frac{1}{T} - \frac{1}{T^\theta}\right)\right) \quad (3)$$

281 where $H(T)$ and H^θ are Henry's constants expressed in mol/m³/Pa at temperature T and T^θ (=
 282 298.15 K), respectively; H^θ equals 7.7×10^{-6} [38]; $d \ln (H)/d(1/T)$ equals 500 K [38] and is the
 283 temperature dependence factor of Henry's constant; and T is the temperature in K.

284 Increasing the agitation speed to 500 rpm effectively improved the gas-liquid mass transfer,
 285 decreasing the H_{2aq} concentration (Fig. 4 and 3B) until reaching values below the theoretical
 286 equilibrium concentration. Similarly, GaR maintained the hydrogen partial pressure of gas
 287 and liquid phase in equilibrium (Fig. 3B).

288 The extent of H_{2aq} accumulation is determined by the HPR and the mass transfer from liquid
 289 to gas phase (Eq. 4) [17,32].

$$290 \quad \frac{dH_{aq}}{dt} = HPR - k_L a (H_{aq} - H_{dis}) \quad (4)$$

291 with H_{2aq} being the hydrogen concentration in the liquid phase [mL/L]; H_{dis} the concentration
 292 of dissolved hydrogen at the thermodynamic equilibrium; HPR the volumetric production of
 293 hydrogen in the liquid phase [mL/L/h]; $k_L a$ the global mass transfer coefficient [1/h] made up
 294 of two terms, i.e. k_L (the "film" coefficient) and a (the specific interfacial area per unit of
 295 liquid volume in the reactor).

296 When the HPR exceeds the gas-liquid mass transfer of the system, H_{2aq} supersaturates.

297 However, elevated H_{2aq} concentrations inhibit the HPR, which again reduce the degree of

298 H_{2aq} supersaturation (Eq. 4) until HPR and H_{2aq} reach an equilibrium. Because of this
299 feedback inhibition, the HPR of a production system is in many cases primarily determined
300 by an insufficient gas-liquid mass transfer instead of the kinetic potential of the culture.

301 The evolution of H_{2aq} accumulation and its dependence on the HPR and the mass transfer
302 was clearly shown in the 3 phases of assay 2A at 300 rpm (Fig. 4A). In the retention phase, a
303 low “HPR post GaR” of $19 (\pm 17)$ mL/L/h (Fig. 3A) was obtained as HPR was strongly affected
304 by the fast retention of hydrogen in the liquid phase (Fig. 4A). The “HPR” during the
305 equilibrium phase was instead higher, reaching $54 (\pm 13)$ mL/L/h (Fig. 3A). Contrary to the
306 “HPR post GaR”, “HPR” was no longer affected by hydrogen retention but rather by the
307 prevalent H_{2aq} of $17.0 (\pm 2.3)$ mL/L, which was determined by the mass transfer of the
308 system (Fig. 3B). The subsequent application of GaR after 2 h removed the accumulated
309 hydrogen from the liquid phase, leading to a high “HPR GaR” of $316 (\pm 54)$ mL/L/h and a
310 decrease of H_{2aq} to $7.5 (\pm 1.0)$ mL/L (Fig. 3A and B). The length of the retention phase was
311 based on the results of assay 2B, where a cultivation at 200 rpm after GaR increased the H_{2aq}
312 to $16.4 (\pm 0.9)$ mL/L in 30 min, i.e. 91% of $18.0 (\pm 0.9)$ mL/L measured after 2 h (Fig. 4B and
313 C). The accumulation of H_{2aq} was, therefore, considered completed at the end of the
314 retention phase and the HPR in equilibrium with H_{2aq} as explained in section 4.1 (Eq. 4). At
315 500 rpm, hydrogen did not accumulate in the liquid phase as demonstrated by the low H_{2aq}
316 of $7.4 (\pm 0.7)$ mL/L after 2 h (Fig. 3B) and the statistically similar values of “HPR post GaR”,
317 HPR” and “HPR GaR”, i.e. $110 (\pm 18)$ mL/L/h (Fig. 3A).

318 In conclusion, at low cell concentrations the sole agitation at 500 rpm as well as GaR
319 provided an adequate mass transfer to remove the produced hydrogen from the liquid to
320 the gas phase and prevent hydrogen supersaturation.

321 **4.2. Enhancement of dark fermentation kinetics**

322 Independent of the technique applied, the reduction of H_{2aq} in assay 2 resulted in a
323 significant increase of the HPR. Adding GaR increased the “HPR” by 94% from 47 (± 8) to 91
324 (± 20) mL/L/h at 200 rpm, whereas increasing the agitation from 300 to 500 rpm enhanced
325 the “HPR” by 107% from 54 (± 13) to 112 (± 22) mL/L/h (Fig. 3A), both accompanied by a
326 simultaneous increase of the GCR.

327 In assay 1, we accelerated the dark fermentation process by using a higher cell concentration
328 (0.79 g CDW/L). At the lowest agitation of 300 rpm, we observed a specific HPR of 294 (± 44)
329 mL H_2 /h/g CDW. Increasing the agitation to 500 rpm accelerated the dark fermentation
330 process, enhancing the specific HPR by 136% to 695 (± 46) mL H_2 /h/g CDW. As observed in
331 assay 2, the higher HPR obtained at 500 rpm was likely due to a decreased H_{2aq}
332 concentration. However, the addition of GaR was capable to further increase the HPR to
333 1090 (± 91) and 1016 (± 22) mL H_2 /h/g CDW at 300 + GaR and 500 + GaR, respectively, i.e.
334 271 and 246% higher than the HPR achieved at 300 rpm in the absence of GaR. This indicates
335 that, in contrast to what was observed at low cell concentrations, 500 rpm agitating was
336 likely insufficient to completely prevent hydrogen supersaturation at high cell
337 concentrations. In contrast, GaR effectively enhanced the gas-liquid mass transfer (by
338 increasing the specific interfacial area a in Eq. 4) and maintained the H_{2aq} low, leading to the
339 highest values of specific HPR. The similar reactor performance at 300 + GaR and 500 + GaR
340 furthermore shows that hydrogen supersaturation was the crucial factor limiting the process
341 as, once it was prevented by GaR, the agitation speed had no influence on the process.

342 The present results are in line with those obtained by Beckers et al. [29], who observed an
343 enhancement of the HPR from 0.14 to 0.26 L/h when agitation was increased from 0 to 400
344 rpm in 2-L reactors using *Clostridium butyricum* at 30°C and glucose as a substrate at a feed

345 concentration of 27.8 mM. However, in that study the H_{2aq} was observed to remain high at
346 approximately 4 times the equilibrium concentration despite 400 rpm agitation.

347 In our experiments, the specific rates of glucose consumption and biomass growth were
348 closely linked to the HPR (Table 3), showing a similar enhancement when the different
349 measures to prevent H_{2aq} supersaturation were applied. The specific GCR and biomass
350 growth rate (BGR) at high cell concentrations increased by 202% and 479% from 4.4 (± 1.3)
351 to 13.3 (± 0.8) mmol glucose/h/g CDW and from 73 (± 11) to 423 (± 9) mg CDW/h/g CDW at
352 300 rpm and 300 rpm + GaR, respectively. This acceleration of the process led to a reduction
353 of the total fermentation time from 11 and 6 h with the sole agitation at 300 and 500 rpm,
354 respectively, to 4 h when GaR was applied independent from the agitation speed.

355 Ljunggren et al. [17] successfully increased the HPR by decreasing H_{2aq} through N_2 headspace
356 sparging using *Caldicellulosiruptor saccharolyticus*. The authors stated that the culture self-
357 regulates the growth rate as a response to high H_{2aq} to slow down the process, decrease the
358 HPR and consequently prevent the H_{2aq} from reaching inhibitory levels (Eq. 4). However, in
359 our study the effect on the specific HPR, BGR and GCR was simultaneous (Fig. 2), indicating
360 that H_{2aq} directly acts on all rates of dark fermentation.

361 **4.3. Hydrogen and biomass yields under different operating conditions and H_{2aq}**

362 **concentrations**

363 Despite the inhibition by H_{2aq} discussed in section 4.2, the HY remained high at 3.0 (± 0.0)
364 mol H_2 /mol glucose (Table 4) when applying 300 rpm agitation without GaR in assay 1. The
365 HY increased even further to 3.5 mol H_2 /mol glucose coupled with a decrease of the LA/AA
366 ratio (Table 4) when GaR maintained the H_{2aq} in equilibrium with the gas phase.

367 *T. neapolitana* predominately ferments glucose via the AA and the LA pathways, with the
368 former leading to hydrogen production and one additional mole of ATP [7].

369 The AA pathway is thereby energetically more challenging [1], because the formation of
370 hydrogen requires a high free Gibbs energy change as protons are poor electron acceptors
371 [39]. The reaction to gaseous hydrogen is favored by low hydrogen concentrations and high
372 temperatures as explained in detail by Verhaart et al. [39]. This indicates that the
373 temperature was most likely responsible for the high HYs at sole agitation of 300 rpm. The
374 additional decrease of H_{2aq} by GaR caused an additional energetical advantage and allowed
375 the further shift towards the AA pathway leading to the increase of the HY.

376 A similar effect on the HY was obtained by Beckers et al. [29], measuring H_{2aq} in 200 mL
377 serum bottles inoculated with *Clostridium butyricum* at 30°C. Unstirred cultures experienced
378 a supersaturation up to 7 times the equilibrium concentration resulting in a reduced HY of
379 1.16 mol H_2 /mol glucose, in comparison to 1.52 mol H_2 /mol glucose obtained when agitating
380 at 120 rpm. The inhibition by hydrogen has also been demonstrated previously in *T.*
381 *neapolitana* cultivation using closed 120 mL serum bottles. d'Ippolito et al. [12] were able to
382 increase the HY by reducing the culture/headspace ratio leading to a lower hydrogen partial
383 pressure in the gas phase.

384 When GaR was applied at high cell concentrations, a lower LA/AA ratio indicates that more
385 energy was gained by the culture per unit of substrate. Concomitantly, a higher BMY was
386 observed, which suggests that biomass production did not, as often assumed, compete with
387 the final product formation, but rather increased simultaneously when the environmental
388 conditions were optimized. The decrease of the biomass concentration at 500 rpm depicted
389 in Fig. 1C was caused by a change of *T. neapolitana* cell morphology in response to nutrient
390 limitations. This phenomenon interferes with the optical density measurement as described
391 in more detail by Dreschke et al. [34], whereas the actual biomass concentration is not
392 affected. In our study, the variation of HY and BMY was much lower than that of HPR under

393 different operating conditions, indicating that hydrogen inhibition primarily acts on the
394 process rates. We assume that a reduction of the dark fermentation rate by the culture at
395 high H_{2aq} concentrations aims to prevent the inhibition of the AA pathway which allows the
396 higher energy yield.

397 **4.4. Biogas recirculation as a strategy to prevent hydrogen supersaturation**

398 A large number of studies used headspace sparging with gases such as N_2 or CO_2 (Table 1) to
399 counteract hydrogen inhibition by lowering H_{dis} (Eq. 4). For instance, Sonnleitner et al. [26]
400 observed an increase of HPR from 25 to 119 mL/L/h when sparging the headspace of a
401 *Caldicellulosiruptor saccharolyticus* culture with N_2 at 1 L/L/h. However, while sparging with
402 external gases is generally successful to improve the process performance (Table 1), it
403 inevitably leads to an undesired dilution of the produced hydrogen and consequently an
404 increase of costs for gas purification. In contrast, the concentration of hydrogen in the
405 produced gas remains high when GaR is applied.

406 To our knowledge, only two studies have so far focused on the recirculation of the H_2 -rich
407 biogas in dark fermentation. Kim et al. [22] used GaR at flow rates ranging from 100 to 400
408 mL/min in a CSTR with a mixed culture at 35°C. They obtained similar HPRs and HYs, i.e.
409 0.77–0.86 and 0.77 mol H_2 / mol hexose, respectively, with and without GaR. This suggests
410 that at the prevalent reactor conditions, hydrogen did not supersaturate in the liquid phase
411 which rendered GaR ineffective. Bakonyi et al. [23] recirculated the internal biogas at two
412 different H_2 concentrations into a CSTR using a mixed culture at 35°C. The recirculation of
413 the less concentrated gas (50% H_2) resulted in a HPR of 8.9 – 9.2, whereas the use of a more
414 concentrated gas (66% H_2) reduced the HPR to 2.7 – 3.0 L H_2 /L/d, compared to 7.4 L H_2 /L/d
415 obtained without recirculation. Unfortunately, a direct measurement of H_{2aq} was not
416 included in any of the two studies, making the correlation of the reactor performance to H_{2aq}

417 impossible. In our study, we directly demonstrate the impact of stirring speed and GaR on
418 H_{2aq} and correlate it to the process performance. GaR has proven highly effective to provide
419 an adequate gas-liquid mass transfer, that can be readily adjusted by adapting the
420 recirculation flow to meet the requirements of the system. Furthermore, the results confirm
421 that maintaining H_{2aq} in equilibrium with the gas phase is sufficient to reach high HY up to
422 3.5 mol H_2 /mol glucose (Table 4) and a high specific HPR of 1090 ± 91 mL/h/g CDW (Table 3).

423 **Conclusions**

424 This study confirms that hydrogen supersaturates in the liquid phase and strongly inhibits
425 dark fermentation by *T. neapolitana cf. capnolactica*. GaR and the sole agitation at 500 rpm
426 efficiently reduced the H_{2aq} (i.e. 30.1 ± 4.4 mL/L) observed at low cell concentration and
427 agitation of 100 rpm to below the equilibrium value suggested by Henry's law (i.e. 9.7 mL/L).
428 At high cell concentrations (i.e. 0.79 g CDW/L), 500 rpm agitation did not provide sufficient
429 gas-liquid mass transfer to prevent H_{2aq} supersaturation, which was instead counteracted by
430 GaR. High H_{2aq} concentrations led to thermodynamic constraints and the reciprocal influence
431 of H_{2aq} and HPR, which directly hampered the dark fermentation rates. In this line, we
432 observed the specific HPR increasing by 271% when adding GaR at 300 rpm, as well as a HY
433 increase from 3.0 to 3.5 mol H_2 /mol glucose. Hence, we conclude that recirculation of H_2 -
434 rich biogas is an efficient method to prevent hydrogen supersaturation and allow high
435 production rates and yields without negatively effecting the hydrogen content of the
436 produced biogas.

437

438 **Funding:** This work was supported by the Marie Skłodowska-Curie European Joint Doctorate
439 (EJD) in Advanced Biological Waste-To-Energy Technologies (ABWET) funded by Horizon
440 2020 under grant agreement no. 643071.

441 **Acknowledgements**

442 The authors want to express their appreciation to the staff of CNR-ICB for the consistent
443 help throughout this study.

444

445

446

447

448

449

450

451

452

453

454

455

456

457

458

459

460

461

462

463

464

465 **Fig. 1:** Glucose consumption (A), cumulative hydrogen production (B) and biomass growth
466 (C) throughout the dark fermentation of 27.8 mM of glucose by *T. neapolitana cf.*
467 *capnolactica* using 300 and 500 rpm agitation speed, excluding or including recirculation of
468 the produced gas (GaR).

469
470 **Fig. 2:** Specific rates of biomass growth (BGR), glucose consumption (GCR) and hydrogen
471 production (HPR) obtained during the dark fermentation of 27.8 mM of glucose by $0.79 (\pm$
472 $0.03)$ g CDW /L of *T. neapolitana cf. capnolactica* using 300 and 500 rpm agitation speed,
473 excluding or including recirculation of the produced gas (GaR). Specific rates were calculated
474 based on the initial biomass concentration in the reactor expressed as cell dry weight (CDW).
475

476 **Fig. 3:** Hydrogen production rate (HPR) (A) and concentration of hydrogen in the liquid phase
477 (H_{2aq}) (B) at different operating conditions using 100, 200, 300 and 500 rpm as well as 200
478 rpm and 500 rpm with gas recirculation (GaR) for 2 h during the dark fermentation of 27.8
479 mM of glucose by *T. neapolitana cf. capnolactica*. (“HPR post GaR” – retention phase, i.e. 25
480 min after applying GaR; “HPR” – equilibrium phase, i.e. 90 min before the subsequent GaR;
481 “HPR GaR” – removal phase, i.e. when applying GaR for 5 min). The dashed line (----)
482 represents the H_{2aq} in equilibrium with the gas phase at 65% H_2 at 80 °C, i.e. 9.7 mL/L.
483

484 **Fig. 4:** Cumulative hydrogen production (●) and H_{2aq} evolution (□) during the dark
485 fermentation of 27.8 mM of glucose by *T. neapolitana cf. capnolactica* under different
486 operating conditions: (A) 100, 300 and 500 rpm agitation speed with 5 min of gas
487 recirculation (GaR) between each condition; (B) and (C) 100, 200 and 200 rpm + GaR. The
488 dashed line (----) represents the H_{2aq} in equilibrium with the gas phase at 65% H_2 at 80 °C, i.e.
489 9.7 mL/L.

490

491

492

493

494

495

496

497

498

499

500

501 **Table 1:** Different techniques applied to decrease the H_{2aq} and reduce its inhibition on dark
502 fermentation. A “x” was used to indicate if H_{2aq} was directly measured in the referenced
503 study or an effect on H_2 yield and production rate was observed.

504

505 **Table 2:** Operating conditions during assay 2. 100, 200, 300 and 500 represent the agitation
506 speed in rpm.

507

508 **Table 3:** Hydrogen production, biomass growth and glucose consumption rates during the
509 dark fermentation of 27.8 mM of glucose by *T. neapolitana cf. capnolactica* at 300 and 500
510 rpm, excluding or including recirculation of the produced gas (GaR). The rates and lag phase
511 were determined through data fitting with a modified Gompertz model. The adequateness
512 of the fit is illustrated by the coefficient of determination (R^2). Specific rates are calculated
513 based on the initial biomass concentration in the reactor.

514

515 **Table 4:** Hydrogen yield (HY), biomass yield (BMY) and glucose consumption obtained in a 2
516 L batch reactor inoculated with 0.79 (\pm 0.03) g CDW/L of *T. neapolitana cf. capnolactica*,
517 performing the dark fermentation of 27.8 mM of glucose at 300 and 500 rpm agitation
518 speed, in the presence or absence of recirculation of the produced gas (GaR).

519

520 **Table 5:** Composition of the digestate at the end of the fermentation of 27.8 mM of glucose
521 by *T. neapolitana cf. capnolactica* using 300 and 500 rpm agitation speed with or without the
522 recirculation of the produced gas (GaR).

523

524 References

525

- 526 [1] Balachandar G, Khanna N, Das D. Biohydrogen production from organic wastes by dark
527 fermentation. In: Biohydrogen. Elsevier; 2013, p. 103–144. doi:10.1016/B978-0-444-
528 59555-3.00006-4.
- 529 [2] Gupta N, Pal M, Sachdeva M, Yadav M, Tiwari A. Thermophilic biohydrogen production
530 for commercial application: The whole picture. Int J Energy Res 2016;40(2):127–45.
531 doi:10.1002/er.3438.
- 532 [3] Show KY, Lee DJ, Tay JH, Lin CY, Chang JS. Biohydrogen production: Current perspectives
533 and the way forward. Int J Hydrogen Energy 2012;37(20):15616–31.
534 doi:10.1016/j.ijhydene.2012.04.109.
- 535 [4] Sinha P, Pandey A. An evaluative report and challenges for fermentative biohydrogen
536 production. Int J Hydrogen Energy 2011;36(13):7460–78.
537 doi:10.1016/j.ijhydene.2011.03.077.
- 538 [5] Wang J, Wan W. Factors influencing fermentative hydrogen production: A review. Int J
539 Hydrogen Energy 2009;34(2):799–811. doi:10.1016/j.ijhydene.2008.11.015.
- 540 [6] Pawar SS, van Niel EWJ. Thermophilic biohydrogen production: how far are we? Appl
541 Microbiol Biotechnol 2013;97(18):7999–8009. doi:10.1007/s00253-013-5141-1.
- 542 [7] Pradhan N, Dipasquale L, d'Ippolito G, Panico A, Lens PNL, Esposito G et al. Hydrogen
543 production by the thermophilic bacterium *Thermotoga neapolitana*. Int J Mol Sci
544 2015;16(6):12578–600. doi:10.3390/ijms160612578.
- 545 [8] Huber R, Hannig M. Thermotogales. In: Dworkin M, Falkow S, Rosenberg E, Schleifer K-
546 H, Stackebrandt E, editors. The Prokaryotes. New York, NY: Springer New York; 2006, p.
547 899–922. doi:10.1007/0-387-30747-8_38.
- 548 [9] Cappelletti M, Bucchi G, Sousa Mendes J de, Alberini A, Fedi S, Bertin L et al.
549 Biohydrogen production from glucose, molasses and cheese whey by suspended and
550 attached cells of four hyperthermophilic *Thermotoga* strains. J Chem Technol
551 Biotechnol 2012;87(9):1291–301. doi:10.1002/jctb.3782.
- 552 [10] Dipasquale L, d'Ippolito G, Gallo C, Vella FM, Gambacorta A, Picariello G et al. Hydrogen
553 production by the thermophilic eubacterium *Thermotoga neapolitana* from storage
554 polysaccharides of the CO₂-fixing diatom *Thalassiosira weissflogii*. Int J Hydrogen Energy
555 2012;37(17):12250–7. doi:10.1016/j.ijhydene.2012.05.160.
- 556 [11] de Vrije T, Budde MA, Lips SJ, Bakker RR, Mars AE, Claassen PA. Hydrogen production
557 from carrot pulp by the extreme thermophiles *Caldicellulosiruptor saccharolyticus* and
558 *Thermotoga neapolitana*. Int J Hydrogen Energy 2010;35(24):13206–13.
559 doi:10.1016/j.ijhydene.2010.09.014.
- 560 [12] d'Ippolito G, Dipasquale L, Vella FM, Romano I, Gambacorta A, Cutignano A et al.
561 Hydrogen metabolism in the extreme thermophile *Thermotoga neapolitana*. Int J
562 Hydrogen Energy 2010;35(6):2290–5. doi:10.1016/j.ijhydene.2009.12.044.
- 563 [13] Dreschke G, Papirio S, Sisinni DMG, Lens PNL, Esposito G. Effect of feed glucose and
564 acetic acid on continuous biohydrogen production by *Thermotoga neapolitana*.
565 Bioresour Technol 2019;273:416–24. doi:10.1016/j.biortech.2018.11.040.
- 566 [14] Nguyen T-AD, Han SJ, Kim JP, Kim MS, Sim SJ. Hydrogen production of the
567 hyperthermophilic eubacterium, *Thermotoga neapolitana* under N₂ sparging condition.
568 Bioresour Technol 2010;101 Suppl 1:41. doi:10.1016/j.biortech.2009.03.041.
- 569 [15] Jayasinghearachchi HS, Sarma PM, Lal B. Biological hydrogen production by extremely
570 thermophilic novel bacterium *Thermoanaerobacter mathranii* A3N isolated from oil

- 571 producing well. Int J Hydrogen Energy 2012;37(7):5569–78.
572 doi:10.1016/j.ijhydene.2011.12.145.
- 573 [16] Kraemer JT, Bagley DM. Supersaturation of dissolved H₂ and CO₂ during fermentative
574 hydrogen production with N₂ sparging. Biotechnol Lett 2006;28(18):1485–91.
575 doi:10.1007/s10529-006-9114-7.
- 576 [17] Ljunggren M, Willquist K, Zacchi G, Van Niel EWJ. A kinetic model for quantitative
577 evaluation of the effect of hydrogen and osmolarity on hydrogen production by
578 *Caldicellulosiruptor saccharolyticus*. Biotechnol Biofuels 2011;4(1):31.
579 doi:10.1186/1754-6834-4-31.
- 580 [18] Zhang Y, Zhang F, Chen M, Chu P-N, Ding J, Zeng RJ. Hydrogen supersaturation in
581 extreme-thermophilic (70°C) mixed culture fermentation. Appl Energy 2013;109:213–9.
582 doi:10.1016/j.apenergy.2013.04.019.
- 583 [19] Kim D-H, Shin H-S, Kim S-H. Enhanced H₂ fermentation of organic waste by CO₂ sparging.
584 Int J Hydrogen Energy 2012;37(20):15563–8. doi:10.1016/j.ijhydene.2012.03.071.
- 585 [20] Lamed RJ, Lobos J. H., Su T. M. Effects of Stirring and Hydrogen on Fermentation
586 Products of *Clostridium thermocellum*. Appl Environ Microbiol 1988:1216–21.
- 587 [21] Nualsri C, Kongjan P, Reungsang A, Imai T. Effect of biogas sparging on the performance
588 of bio-hydrogen reactor over a long-term operation. PLoS ONE 2017;12(2):e0171248.
589 doi:10.1371/journal.pone.0171248.
- 590 [22] Kim D, Han S, Kim S, Shin H. Effect of gas sparging on continuous fermentative hydrogen
591 production. Int J Hydrogen Energy 2006;31(15):2158–69.
592 doi:10.1016/j.ijhydene.2006.02.012.
- 593 [23] Bakonyi P, Buitrón G, Valdez-Vazquez I, Nemestóthy N, Bélafi-Bakó K. A novel gas
594 separation integrated membrane bioreactor to evaluate the impact of self-generated
595 biogas recycling on continuous hydrogen fermentation. Appl Energy 2017;190:813–23.
596 doi:10.1016/j.apenergy.2016.12.151.
- 597 [24] Kraemer JT, Bagley DM. Optimisation and design of nitrogen-sparged fermentative
598 hydrogen production bioreactors. Int J Hydrogen Energy 2008;33(22):6558–65.
599 doi:10.1016/j.ijhydene.2008.08.033.
- 600 [25] Mandal B, Nath K, Das D. Improvement of biohydrogen production under decreased
601 partial pressure of H₂ by *Enterobacter cloacae*. Biotechnol Lett 2006;28(11):831–5.
602 doi:10.1007/s10529-006-9008-8.
- 603 [26] Sonnleitner A, Peintner C, Wukovits W, Friedl A, Schnitzhofer W. Process investigations
604 of extreme thermophilic fermentations for hydrogen production: effect of bubble
605 induction and reduced pressure. Bioresour Technol 2012;118:170–6.
606 doi:10.1016/j.biortech.2012.05.046.
- 607 [27] Zhang F, Zhang Y, Chen M, Zeng RJ. Hydrogen supersaturation in thermophilic mixed
608 culture fermentation. Int J Hydrogen Energy 2012;37(23):17809–16.
609 doi:10.1016/j.ijhydene.2012.09.019.
- 610 [28] Fritsch M, Hartmeier W, Chang J. Enhancing hydrogen production of *Clostridium*
611 *butyricum* using a column reactor with square-structured ceramic fittings. Int J
612 Hydrogen Energy 2008;33(22):6549–57. doi:10.1016/j.ijhydene.2008.07.070.
- 613 [29] Beckers L, Masset J, Hamilton C, Delvigne F, Toye D, Crine M et al. Investigation of the
614 links between mass transfer conditions, dissolved hydrogen concentration and
615 biohydrogen production by the pure strain *Clostridium butyricum* CWBI1009. Biochem
616 Eng J 2015;98:18–28. doi:10.1016/j.bej.2015.01.008.
- 617 [30] Obazu FO, Ngoma L, Gray VM. Interrelationships between bioreactor volume, effluent
618 recycle rate, temperature, pH, %H₂, hydrogen productivity and hydrogen yield with

- 619 undefined bacterial cultures. *Int J Hydrogen Energy* 2012;37(7):5579–90.
620 doi:10.1016/j.ijhydene.2012.01.001.
- 621 [31] Dreschke G, Papirio S, Lens PN, Esposito G. Influence of liquid-phase hydrogen on dark
622 fermentation by *Thermotoga neapolitana*. *Renew Energy* 2019;140:354–60.
623 doi:10.1016/j.renene.2019.02.126.
- 624 [32] Paus A, Andre G, Perrier M, Guiot SR. Liquid-to-gas mass transfer in anaerobic
625 processes: Inevitable transfer limitations of methane and hydrogen in the
626 biomethanation process. *Appl Environ Microbiol* 1990;56(6):1636–44.
- 627 [33] Pradhan N, Dipasquale L, d'Ippolito G, Panico A, Lens PN, Esposito G et al. Hydrogen and
628 lactic acid synthesis by the wild-type and a laboratory strain of the hyperthermophilic
629 bacterium *Thermotoga neapolitana* DSMZ 4359 T under capnophilic lactic fermentation
630 conditions. *Int J Hydrogen Energy* 2017;42(25):16023–30.
631 doi:10.1016/j.ijhydene.2017.05.052.
- 632 [34] Dreschke G, d'Ippolito G, Panico A, Lens PNL, Esposito G, Fontana A. Enhancement of
633 hydrogen production rate by high biomass concentrations of *Thermotoga neapolitana*.
634 *Int J Hydrogen Energy* 2018. doi:10.1016/j.ijhydene.2018.05.072.
- 635 [35] Bernfeld P. Amylases, α and β . In: Chance B, editor. Preparation and assay of enzymes.
636 San Diego, Calif.: Acad. Press; 1955, p. 149–158.
- 637 [36] Mancini G, Papirio S, Lens PN, Esposito G. Increased biogas production from wheat
638 straw by chemical pretreatments. *Renew Energy* 2018;119:608–14.
639 doi:10.1016/j.renene.2017.12.045.
- 640 [37] Bastidas-Oyanedel J-R, Mohd-Zaki Z, Zeng RJ, Bernet N, Pratt S, Steyer J-P et al. Gas
641 controlled hydrogen fermentation. *Bioresour Technol* 2012;110:503–9.
642 doi:10.1016/j.biortech.2012.01.122.
- 643 [38] Sander R. Compilation of Henry's law constants (version 4.0) for water as solvent. *Atmos*
644 *Chem Phys* 2015;15(8):4399–981. doi:10.5194/acp-15-4399-2015.
- 645 [39] Verhaart MRA, Bielen AAM, van der Oost J, Stams AJM, Kengen SWM. Hydrogen
646 production by hyperthermophilic and extremely thermophilic bacteria and archaea:
647 Mechanisms for reductant disposal. *Environ Technol* 2010;31(8-9):993–1003.
648 doi:10.1080/09593331003710244.

1 **H₂-rich biogas recirculation prevents hydrogen supersaturation and enhances**
2 **hydrogen production by *Thermotoga neapolitana* cf. *capnolactica***

3 Gilbert Dreschke^{a, b, *}, Stefano Papirio^c, Giuliana d'Ippolito^b, Antonio Panico^d, Piet N.L. Lens^e,

4 Giovanni Esposito^a, Angelo Fontana^b

5

6 ^aDepartment of Civil and Mechanical Engineering, University of Cassino and Southern Lazio,

7 Via Di Biasio, 43, 03043 Cassino, FR, Italy. (E-mail: giovanni.esposito@unicas.it)

8 ^bBio-Organic Chemistry Unit, Institute of Biomolecular Chemistry, Italian National Council of

9 Research, Via Campi Flegrei 34, 80078 Pozzuoli, NA, Italy. (E-mails: gdippolito@icb.cnr.it,

10 afontana@icb.cnr.it)

11 ^cDepartment of Civil, Architectural and Environmental Engineering, University of Napoli

12 Federico II, Via Claudio 21, 80125 Napoli, Italy. (stefano.papirio@unina.it)

13 ^dTelematic University Pegaso, Piazza Trieste e Trento, 48, 80132, Napoli, Italy. (E-mail:

14 antonio.panico@unipegaso.it)

15 ^eUNESCO - IHE Institute for Water Education, Westvest 7, 2611-AX Delft, The Netherlands.

16 (E-mail: p.lens@unesco-ihe.org)

17

18

19 * Corresponding author

20 Gilbert Dreschke MSc

21 Present address:

22 Department of Civil and Mechanical Engineering, University of Cassino and Southern Lazio,

23 Via Di Biasio 43, 03043 Cassino, FR, Italy

24 Email: g.dreschke@unicas.it

25 **Abstract**

26 This study focused on the supersaturation of hydrogen in the liquid phase (H_{2aq}) and its
27 inhibitory effect on dark fermentation by *Thermotoga neapolitana* cf. *capnolactica* by
28 increasing the agitation (from 100 to 500 rpm) and recirculating H_2 -rich biogas (GaR). At low
29 cell concentrations, both 500 rpm and GaR reduced the H_{2aq} from 30.1 (\pm 4.4) mL/L to the
30 lowest values of 7.4 (\pm 0.7) mL/L and 7.2 (\pm 1.2) mL/L, respectively. However, at high cell
31 concentrations (0.79 g CDW/L), the addition of GaR at 300 rpm was more efficient and
32 increased the hydrogen production rate by 271%, compared to a 136% increase when raising
33 the agitation to 500 rpm instead. While H_{2aq} primarily affected the dark fermentation rate,
34 GaR concomitantly increased the hydrogen yield up to 3.5 mol H_2 /mol glucose. Hence, H_{2aq}
35 supersaturation highly depends on the systems gas-liquid mass transfer and strongly inhibits
36 dark fermentation.

37

38

39

40

41

42

43

44

45 **Key words:** *Thermotoga neapolitana*; Dark fermentation; Gas recirculation; Sparging;
46 Hydrogen supersaturation; End product inhibition

47

48 Declarations of interest: none

49 **Highlights**

- 50 • H₂ supersaturates in the liquid phase at 100 rpm despite hyperthermophilic
51 conditions.
- 52 • High H_{2aq} concentrations directly inhibit the specific rates of dark fermentation.
- 53 • H₂ supersaturation and H₂ production rate depend on the gas-liquid mass transfer.
- 54 • H₂-rich biogas recirculation is an effective method to prevent H₂ supersaturation.
- 55 • Gas recirculation increased the hydrogen production rate by 271%.

56

57

58

59

60 **Abbreviations**

61 AA acetic acid

62 BGR biomass growth rate

63 BMY biomass yield

64 CSTR continuously stirred tank reactor

65 GaR recirculation of H₂-rich biogas

66 GCR glucose consumption rate

67 H_{2aq} liquid phase hydrogen

68 HPR hydrogen production rate

69 HY hydrogen yield

70 LA lactic acid

71 1. Introduction

72 Hydrogen, a nonpolluting energy carrier can be produced from organic residues in an
73 environmental-friendly biological process called dark fermentation [1,2]. Hydrogen
74 production has been reported in a wide range of temperatures, with thermophilic conditions
75 being generally correlated to higher hydrogen yields (HY) [1,2]. A variety of microbial species
76 are capable of fermentative hydrogen production [3] in both mixed and pure culture
77 applications [4]. The use of mixed cultures is considered to be the simpler and have a more
78 practical approach [4], but often entailing the coexistence of microorganisms which do not
79 produce or even consume hydrogen [5].

80 *Thermotoga neapolitana* (hereafter *T. neapolitana*) is a hyperthermophilic microorganism
81 with a high potential for hydrogen production via dark fermentation [6,7]. Some of the key
82 characteristics exhibited by this organism include fast growth kinetics [7], and efficient
83 degradation of a wide range of substrates, e.g. glucose, fructose, xylose, maltose, starch
84 [7,8], molasses, cheese whey [9], algal biomass [10], and carrot pulp [11]. *T. neapolitana* is
85 capable to approach the theoretical HY of 4 mol H₂/mol glucose by optimizing the conditions
86 for the hydrogen forming acetate pathway [12,13]. Additionally, the hyperthermophilic
87 culture conditions of *T. neapolitana* further stimulate the reaction rates [2] and hamper the
88 growth competitive microorganisms [14], also leading to a pasteurization of the used
89 substrate [15].

90 In dark fermentative hydrogen production, the presence of hydrogen is one of the most
91 crucial factors, as high concentrations of hydrogen are a major inhibitor of the process. To
92 reduce the inhibitory effect of hydrogen on the process, previous experimental studies
93 (Table 1) have employed a variety of techniques, e.g. sparging the headspace, reducing the
94 total pressure, applying vigorous stirring, optimizing the reactor design, or simply increasing

95 the headspace/solution ratio [12]. Regardless of the method used, alleviation of hydrogen
96 inhibition results in increased HYs and/or hydrogen production rates (HPR).
97 The headspace hydrogen concentration has been widely used (Table 1) to predict hydrogen
98 in the liquid phase (H_{2aq}), which *de facto* acts on the microbial cultures. However, poorly
99 soluble gases, such as hydrogen, supersaturate in solution during anaerobic processes
100 [31,32]. Studies, including a direct measurement of H_{2aq} (Table 1), have observed that H_{2aq}
101 can exceed the equilibrium concentration suggested by Henry's law multiple times. As a
102 result, the measurement of headspace hydrogen is considered inappropriate to predict the
103 H_{2aq} value [2,16–18,31,32].

104 Our study focused on the effect of agitation and biogas recirculation on the accumulation of
105 H_{2aq} and the consequent impact on dark fermentation by *T. neapolitana*. The main goal was
106 to demonstrate that the recirculation of the H_2 -rich biogas (GaR) into the culture broth is an
107 effective method to improve the gas-liquid mass transfer and prevent H_{2aq} from
108 supersaturating, without diluting the H_2 percentage in the biogas. Furthermore, we wanted
109 to show that keeping the H_{2aq} in equilibrium with the gas phase is sufficient to achieve high
110 hydrogen production yields and rates. In a first assay, the effect of GaR and agitation speed
111 on hydrogen production was evaluated using a highly concentrated *T. neapolitana* culture. In
112 a second assay, a direct measurement of H_{2aq} was included to demonstrate the correlation
113 between hydrogen supersaturation and the performance of dark fermentation.

114

115 2. Material and methods

116 2.1. Bacterial culture and medium

117 A pure culture of *Thermotoga neapolitana* cf. *capnolactica* [33] was used in all experiments.
118 The cultivation and storage conditions for the culture, the preparation of inoculum for
119 elevated cell concentrations (assay 1) and the modified ATCC 1977 medium used (containing
120 27.8 mM of glucose) were as described by Dreschke et al. [34]. The pH of the medium was
121 adjusted to 7.5 prior to being autoclaved at 110 °C for 5 min. Prior to the inoculation, the
122 medium was heated at 80 °C for 30 min and sparged with N₂ for 5 min to remove the
123 dissolved oxygen.

124 2.2. Experimental design

125 All experiments were run in a 3-L fully controlled continuously stirred tank reactor (CSTR)
126 (Applikon Biotechnology, the Netherlands) with a working volume of 2 L. The operating
127 temperature was kept at a constant 80 °C and pH was automatically adjusted to 7 by adding
128 1M NaOH. GaR was applied by continuously pumping the produced biogas from the
129 headspace to a gas dispersion device at the base of the reactor at a flow rate of 350 mL/min.
130 The produced biogas was released into 500 mL water displacement systems to avoid
131 pressure build-up and quantified every hour. Liquid samples of 2 mL were withdrawn each
132 30 or 60 min. The fermentation was considered completed when the reactors ceased to
133 produce biogas. Fermentation time was approximated from the inoculation to the end of the
134 fermentation. Each condition was conducted in duplicate to demonstrate reproducibility.

135 2.2.1. Assay 1 – Effect of agitation speed and gas recirculation on dark 136 fermentation at high cell concentrations

137 Assay 1 was designed to study the effect of GaR and agitation speed on the dark
138 fermentation process at high cell concentrations of *T. neapolitana*. The reactor was
139 inoculated with 80 mL of concentrated inoculum [34] resulting in a biomass concentration of
140 0.79 (\pm 0.03) g cell dry weight (CDW)/L. The following operating conditions were
141 investigated: 300 rpm agitation (300); 300 rpm agitation with gas recirculation (300 + GaR);
142 500 rpm agitation (500); 500 rpm agitation with gas recirculation (500 + GaR).

143 **2.2.2. Assay 2 – Effect of GaR and agitation speed on H_{2aq}**

144 Assays 2A and 2B were designed to study the effect of agitation speed and GaR on the
145 retention of hydrogen in the liquid phase and its influence on the dark fermentation process.
146 The reactor was inoculated with 20 mL of storage culture (1% v/v) and maintained for 15 h
147 at 100 rpm to acclimatize the culture. Afterwards, a sequence of operating conditions was
148 used with each condition being operated for 2 h as described in Table 2. In assay 2A, 5 min of
149 500 rpm + GaR (Table 2 – shaded grey cells) was used before each operating condition to
150 remove the accumulated hydrogen from the liquid phase. After 5 or 30 min and at the end
151 of each operating condition, 20 mL of broth was withdrawn to monitor H_{2aq}.

152 **2.3. Analytical Methods**

153 **2.3.1. Assay 1**

154 Cell growth was determined by measuring spectrophotometrically (Lambda 365, Perkin
155 Elmer, USA) optical density (OD₅₄₀) of the liquid samples at 540 nm. Liquid samples were
156 centrifuged at 10,000 rpm for 5 min to collect the supernatant for the **determination of**
157 **glucose**, acetic acid (AA), lactic acid (LA) and alanine concentration as described by Dreschke
158 et al. [34]. The glucose concentration was measured by the dinitrosalicylic acid method [35],
159 while AA, LA and alanine were quantified by ¹H Nuclear Magnetic Resonance (NMR) with a

160 600 MHz spectrometer (Bruker Avance 400) as described by Dipasquale et al. [10]. After the
161 completion of the fermentation, 500 mL of culture broth was centrifuged at 3750 rpm for 20
162 min for the determination of CDW via freeze drying. The concentration of hydrogen in the
163 produced gas was analyzed by gas chromatography as described by Dipasquale et al. [10].
164 The conversion from volumetric to molar H₂ production was performed using the ideal gas
165 law.

166 **2.3.2. Assay 2**

167 Glucose, AA and LA concentrations were determined using an HPLC (Prominence LC-20A
168 Series, Shimadzu, Japan), equipped with UV/Vis (SPD-20A, Shimadzu Japan) and refractive
169 index (RID-20A, Shimadzu, Japan) detectors, with the method described by Mancini et al.
170 [36] with 0.0065 M of sulfuric acid as the mobile phase. The concentration of hydrogen in
171 the biogas was determined with a Varian 3400 gas chromatograph (GC), equipped with a
172 thermal conductivity detector (TCD) and a Restek packed column using argon as the carrier
173 gas.

174 For the determination of H_{2aq}, a modified method of Kraemer and Bagley [16,17,37] was
175 applied. Vials with a total volume of 31 mL were closed with silicon septa and depressurized
176 using a plastic syringe. 20 mL of sample was injected into the vials and immediately placed
177 upside down in **in fridge** to equilibrate the liquid and the gas phases. After around 20 h, the
178 sample was heated at room temperature and the negative pressure equilibrated by adding
179 air to the gas phase of the sample. The concentration of hydrogen in the gas phase was
180 measured by the GC described above and referred to the 20 mL of liquid sample.

181 **2.4. Kinetic study of dark fermentation**

182 The rates and lag phases of dark fermentation were evaluated in terms of biomass growth,
183 hydrogen production and glucose consumption and calculated by fitting the experimental
184 data with a modified Gompertz model as described by Dreschke et al. [34].

185 **2.5. Statistical analysis**

186 The statistical significance of the experimental data was determined by the calculation of the
187 p-value applying an unpaired t-test with Microsoft Excel 2016 (Microsoft Corporation, USA).

188 **3. Results**

189 **3.1. Effect of agitation speed and GaR on dark fermentation at high cell concentrations** 190 **(assay 1)**

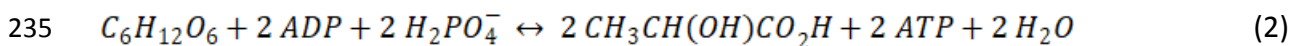
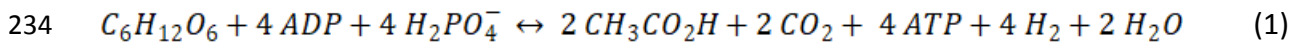
191 Fig. 1. shows the glucose consumption (A), cumulative hydrogen (B) and biomass growth (C)
192 during batch fermentation with an initial cell concentration of $0.79 (\pm 0.03)$ g CDW/L of *T.*
193 *neapolitana* using an agitation of 300 or 500 rpm with and without GaR.
194 Increasing the agitation significantly enhanced the specific rates of biomass growth [mg
195 CDW/h/g CDW], hydrogen production [mL H₂/h/g CDW], and glucose consumption [mmol
196 glucose/h/g CDW] from $73 (\pm 11)$, $294 (\pm 44)$, and $4.4 (\pm 1.3)$ at 300 rpm to $266 (\pm 9)$ (p-value:
197 0.003), $695 (\pm 46)$ (p-value: 0.012), and $10.1 (\pm 0.6)$ (p-value: 0.028) at 500 rpm (Fig. 2, Table
198 3), respectively. Due to the accelerated process, the fermentation time and lag phase of
199 hydrogen production were reduced from 11 h and $2.9 (\pm 0.2)$ h at 300 rpm to 6 h and from
200 $1.3 (\pm 0.1)$ h at 500 rpm (Table 3), respectively. The HY increased from $3.0 (\pm 0.0)$ at 300 rpm
201 to $3.2 (\pm 0.1)$ mol H₂/mol glucose at 500 rpm, while the biomass yield (BMY) increased from
202 approximately 16.7 to 21.9 g CDW/mol glucose (Table 4). The composition of the end
203 products, expressed in terms of an LA/AA ratio, decreased from 0.31 at 300 rpm to 0.21 at
204 500 rpm (Table 5).

205 A combination of GaR and agitation speed at 300 rpm further accelerated the dark
206 fermentation. The specific biomass growth rate reached $423 (\pm 9)$ mg CDW/h/g CDW (p -
207 value: 0.004), while the specific rates of hydrogen production and glucose consumption
208 increased up to $1090 (\pm 91)$ mL/h/g CDW (p -value: 0.032) and $13.3 (\pm 0.8)$ mmol glucose/h/g
209 CDW (p -value: 0.040), respectively, over those obtained at 500 rpm without GaR (Fig. 2,
210 Table 3). The fermentation was completed within 4 h with a lag phase of $0.4 (\pm 0.0)$ h (Table
211 3), a HY of $3.5 (\pm 0.2)$ mol H₂/mol glucose, an approximate BMY of 24.8 g CDW/mol glucose
212 (Table 4), and a LA/AA ratio of 0.11 (Table 5).

213 Increasing the agitation to 500 rpm while applying GaR had no significant effect on the
214 process, as shown by the similar performance obtained at 300 rpm + GaR and 500 rpm + GaR
215 (Fig. 1). At 500 rpm + GaR, the specific rates of biomass growth, hydrogen production and
216 glucose consumption were $431 (\pm 9)$ mg CDW/h/g CDW, $1016 (\pm 22)$ mL H₂/h/g CDW and
217 $12.7 (\pm 0.2)$ mmol glucose/h/g CDW (Fig. 2, Table 3), respectively. The HY reached $3.3 (\pm 0.1)$
218 mol H₂/mol glucose (Table 4) coupled with a LA/AA ratio of 0.13 (Table 5). The fermentation
219 time and lag phase of hydrogen production remained at 4 h and $0.5 (\pm 0.1)$ h (Table 3),
220 respectively, with an approximate BMY of 27.7 g CDW/mol glucose.

221 The highest volumetric HPRs of $850 (\pm 71)$ and $813 (\pm 18)$ mL/h/L were obtained when GaR
222 was applied at 300 and 500 rpm, respectively (Table 3). The hydrogen concentration in the
223 biogas produced was not affected by the use of GaR or the agitation speed and remained
224 constant at $65 (\pm 2)\%$ (data not shown) under all studied conditions. In all bioassays, glucose
225 was consumed up to 82 - 89 % (Table 4) with AA and LA as the main fermentation end
226 products in the digestate and alanine constituting a minor proportion of 2% (Table 5). A
227 mass balance based on the stoichiometric equations 1 and 2 was performed to validate the
228 experimental results. The dark fermentation model suggests the formation of two moles of

229 fermentation end products (AA and LA) per mole of glucose with the concomitant
230 production of 2 moles of hydrogen per mole of AA. Under all operating conditions, the sum
231 of fermentation products in the digestate reached 92% or more of the theoretical value
232 calculated from the glucose consumption and 2.08 (± 0.01) moles H₂ per mole of AA were
233 averagely produced.



236

237 **3.2. Effect of GaR and agitation speed on H_{2aq} and HPR (assay 2)**

238 **3.2.1. Assay 2A – Use of different agitation speeds**

239 Assay 2A assessed the effect of the agitation speed on H_{2aq} and HPR. After the initial 15 h at
240 100 rpm, H_{2aq} accumulated up to 30.1 (± 4.4) mL/L (Fig. 3B). Then, using 500 rpm + GaR for 5
241 min before each operating condition reduced H_{2aq} to an average of 7.5 (± 1.0) mL/L (Fig. 4A).
242 The subsequent agitation of the culture at 300 and 500 rpm without GaR for 2 h led to a H_{2aq}
243 of 17.0 (± 2.3) and 7.4 (± 0.7) mL/L, respectively (Fig. 3B).

244 To better demonstrate the effect of hydrogen retention in the liquid phase on the HPR, the 2
245 h duration of each operating condition was subdivided in 3 phases and the HPR was
246 calculated for each individual phase: 1 – removal phase, i.e. period from 0 to 5 min after
247 changing the operating condition when additional GaR was applied (“HPR GaR”); 2 –
248 retention phase, i.e. period from 5 to 30 min after changing the operating condition (“HPR
249 post GaR”); 3 – equilibrium phase, i.e. period from 30 to 120 min after changing the
250 operating condition (“HPR”) (Fig. 3A). At 300 rpm, a significantly higher “HPR GaR” of 316 (\pm
251 54) mL/L/h (Fig. 3A) was observed than “HPR” of 54 (± 13) mL/L/h (p-value: 0.0002) and

252 “HPR post GaR” of $19 (\pm 17)$ mL/L/h (p-value: 0.0017), respectively. In contrast, at 500 rpm,
253 the HPR remained similar before, during, and after GaR. The “HPR” reached $112 (\pm 22)$
254 mL/L/h, which was not significantly different from “HPR post GaR” ($100 (\pm 16)$ mL/L/h, p-
255 value: 0.397) and “HPR GaR” ($120 (\pm 11)$ mL/L/h, p-value: 0.614) (Fig. 3A). Changing the
256 agitation from 300 to 500 rpm roughly doubled the “HPR”, and concomitantly increased the
257 glucose consumption rate (GCR) from $3.6 (\pm 0.4)$ to $4.7 \pm (0.3)$ mmol/L/h (p-value: 0.016)
258 (data not shown).

259 **3.2.2. Assay 2B – Gas sparging**

260 Assay 2B was run to assess the effect of GaR on H_{2aq} and HPR at a constant agitation at 200
261 rpm. Similar to assay 2A, the highest H_{2aq} of $26.8 (\pm 3.6)$ mL/L (Fig. 4B and C) was obtained
262 after 15 h of operation at 100 rpm. Applying 200 rpm + GaR rapidly decreased the H_{2aq} to 9.0
263 (± 1.8) mL/L in 5 min (Fig. 4B and C) reaching a final value of $7.2 (\pm 1.2)$ mL/L after 2 h (Fig.
264 4B). The 200-rpm agitation without GaR caused an accumulation of H_{2aq} up to a
265 concentration of $16.4 (\pm 0.9)$ mL/L in 30 min, which was 91% of $18.0 (\pm 0.9)$ mL/L reached
266 after 2 h (Fig. 4B and C). The “HPR” at 200 rpm + GaR of $91 (\pm 20)$ mL/L/h was significantly
267 higher than $47 (\pm 8)$ mL/L/h (p-value: 0.017) obtained at 200 rpm without GaR (Fig. 3A).
268 Concomitantly, the GCR reached values of $4.2 (\pm 0.1)$ and $3.1 (\pm 0.8)$ mmol/L/h (p-value:
269 0.077), at 200 rpm + GaR and 200 rpm without GaR, respectively (data of GCR not shown).
270 When agitation was increased from 100 to 200 rpm after 15 h in the absence of GaR, H_{2aq}
271 decreased from 29.4 to 24.8 mL/L in 2 h (Fig. 4C), which was higher than $18.7 (\pm 4.6)$ mL/L
272 obtained at 200 rpm agitation at 21 h after applying GaR between 17 and 19 h.

273 **4. Discussion**

274 **4.1. Effect of agitation speed and gas recirculation on H_{2aq} concentration**

275 In this study, GaR and agitation speed were examined as strategies to lower H_{2aq} and, thus,
 276 stimulate H_2 production by *T. neapolitana*. Agitating at 100 rpm led to the highest H_{2aq} ,
 277 i.e. 30.1 (\pm 4.4) mL/L, which was approximately 3 times higher than the theoretical dissolved
 278 hydrogen concentration (i.e. 9.7 mL/L) in equilibrium with a gas phase containing 65% H_2 at
 279 80 °C according to Henry's Law (Eq. 3):

$$280 \quad H(T) = H^\theta * \exp\left(\frac{d \ln(H)}{d(1/T)} * \left(\frac{1}{T} - \frac{1}{T^\theta}\right)\right) \quad (3)$$

281 where $H(T)$ and H^θ are Henry's constants expressed in mol/m³/Pa at temperature T and T^θ (=
 282 298.15 K), respectively; H^θ equals 7.7×10^{-6} [38]; $d \ln (H)/d(1/T)$ equals 500 K [38] and is the
 283 temperature dependence factor of Henry's constant; and T is the temperature in K.

284 Increasing the agitation speed to 500 rpm effectively improved the gas-liquid mass transfer,
 285 decreasing the H_{2aq} concentration (Fig. 4 and 3B) until reaching values below the theoretical
 286 equilibrium concentration. Similarly, GaR maintained the hydrogen partial pressure of gas
 287 and liquid phase in equilibrium (Fig. 3B).

288 The extent of H_{2aq} accumulation is determined by the HPR and the mass transfer from liquid
 289 to gas phase (Eq. 4) [17,32].

$$290 \quad \frac{dH_{aq}}{dt} = HPR - k_L a (H_{aq} - H_{dis}) \quad (4)$$

291 with H_{2aq} being the hydrogen concentration in the liquid phase [mL/L]; H_{dis} the concentration
 292 of dissolved hydrogen at the thermodynamic equilibrium; HPR the volumetric production of
 293 hydrogen in the liquid phase [mL/L/h]; $k_L a$ the global mass transfer coefficient [1/h] made up
 294 of two terms, i.e. k_L (the "film" coefficient) and a (the specific interfacial area per unit of
 295 liquid volume in the reactor).

296 When the HPR exceeds the gas-liquid mass transfer of the system, H_{2aq} supersaturates.

297 However, elevated H_{2aq} concentrations inhibit the HPR, which again reduce the degree of

298 H_{2aq} supersaturation (Eq. 4) until HPR and H_{2aq} reach an equilibrium. Because of this
299 feedback inhibition, the HPR of a production system is in many cases primarily determined
300 by an insufficient gas-liquid mass transfer instead of the kinetic potential of the culture.

301 The evolution of H_{2aq} accumulation and its dependence on the HPR and the mass transfer
302 was clearly shown in the 3 phases of assay 2A at 300 rpm (Fig. 4A). In the retention phase, a
303 low “HPR post GaR” of $19 (\pm 17)$ mL/L/h (Fig. 3A) was obtained as HPR was strongly affected
304 by the fast retention of hydrogen in the liquid phase (Fig. 4A). The “HPR” during the
305 equilibrium phase was instead higher, reaching $54 (\pm 13)$ mL/L/h (Fig. 3A). Contrary to the
306 “HPR post GaR”, “HPR” was no longer affected by hydrogen retention but rather by the
307 prevalent H_{2aq} of $17.0 (\pm 2.3)$ mL/L, which was determined by the mass transfer of the
308 system (Fig. 3B). The subsequent application of GaR after 2 h removed the accumulated
309 hydrogen from the liquid phase, leading to a high “HPR GaR” of $316 (\pm 54)$ mL/L/h and a
310 decrease of H_{2aq} to $7.5 (\pm 1.0)$ mL/L (Fig. 3A and B). The length of the retention phase was
311 based on the results of assay 2B, where a cultivation at 200 rpm after GaR increased the H_{2aq}
312 to $16.4 (\pm 0.9)$ mL/L in 30 min, i.e. 91% of $18.0 (\pm 0.9)$ mL/L measured after 2 h (Fig. 4B and
313 C). The accumulation of H_{2aq} was, therefore, considered completed at the end of the
314 retention phase and the HPR in equilibrium with H_{2aq} as explained in section 4.1 (Eq. 4). At
315 500 rpm, hydrogen did not accumulate in the liquid phase as demonstrated by the low H_{2aq}
316 of $7.4 (\pm 0.7)$ mL/L after 2 h (Fig. 3B) and the statistically similar values of “HPR post GaR”,
317 HPR” and “HPR GaR”, i.e. $110 (\pm 18)$ mL/L/h (Fig. 3A).

318 In conclusion, at low cell concentrations the sole agitation at 500 rpm as well as GaR
319 provided an adequate mass transfer to remove the produced hydrogen from the liquid to
320 the gas phase and prevent hydrogen supersaturation.

321 **4.2. Enhancement of dark fermentation kinetics**

322 Independent of the technique applied, the reduction of H_{2aq} in assay 2 resulted in a
323 significant increase of the HPR. Adding GaR increased the “HPR” by 94% from 47 (± 8) to 91
324 (± 20) mL/L/h at 200 rpm, whereas increasing the agitation from 300 to 500 rpm enhanced
325 the “HPR” by 107% from 54 (± 13) to 112 (± 22) mL/L/h (Fig. 3A), both accompanied by a
326 simultaneous increase of the GCR.

327 In assay 1, we accelerated the dark fermentation process by using a higher cell concentration
328 (0.79 g CDW/L). At the lowest agitation of 300 rpm, we observed a specific HPR of 294 (± 44)
329 mL H_2 /h/g CDW. Increasing the agitation to 500 rpm accelerated the dark fermentation
330 process, enhancing the specific HPR by 136% to 695 (± 46) mL H_2 /h/g CDW. As observed in
331 assay 2, the higher HPR obtained at 500 rpm was likely due to a decreased H_{2aq}
332 concentration. However, the addition of GaR was capable to further increase the HPR to
333 1090 (± 91) and 1016 (± 22) mL H_2 /h/g CDW at 300 + GaR and 500 + GaR, respectively, i.e.
334 271 and 246% higher than the HPR achieved at 300 rpm in the absence of GaR. This indicates
335 that, in contrast to what was observed at low cell concentrations, 500 rpm agitating was
336 likely insufficient to completely prevent hydrogen supersaturation at high cell
337 concentrations. In contrast, GaR effectively enhanced the gas-liquid mass transfer (by
338 increasing the specific interfacial area a in Eq. 4) and maintained the H_{2aq} low, leading to the
339 highest values of specific HPR. The similar reactor performance at 300 + GaR and 500 + GaR
340 furthermore shows that hydrogen supersaturation was the crucial factor limiting the process
341 as, once it was prevented by GaR, the agitation speed had no influence on the process.

342 The present results are in line with those obtained by Beckers et al. [29], who observed an
343 enhancement of the HPR from 0.14 to 0.26 L/h when agitation was increased from 0 to 400
344 rpm in 2-L reactors using *Clostridium butyricum* at 30°C and glucose as a substrate at a feed

345 concentration of 27.8 mM. However, in that study the H_{2aq} was observed to remain high at
346 approximately 4 times the equilibrium concentration despite 400 rpm agitation.
347 In our experiments, the specific rates of glucose consumption and biomass growth were
348 closely linked to the HPR (Table 3), showing a similar enhancement when the different
349 measures to prevent H_{2aq} supersaturation were applied. The specific GCR and biomass
350 growth rate (BGR) at high cell concentrations increased by 202% and 479% from 4.4 (± 1.3)
351 to 13.3 (± 0.8) mmol glucose/h/g CDW and from 73 (± 11) to 423 (± 9) mg CDW/h/g CDW at
352 300 rpm and 300 rpm + GaR, respectively. This acceleration of the process led to a reduction
353 of the total fermentation time from 11 and 6 h with the sole agitation at 300 and 500 rpm,
354 respectively, to 4 h when GaR was applied independent from the agitation speed.
355 Ljunggren et al. [17] successfully increased the HPR by decreasing H_{2aq} through N_2 headspace
356 sparging using *Caldicellulosiruptor saccharolyticus*. The authors stated that the culture self-
357 regulates the growth rate as a response to high H_{2aq} to slow down the process, decrease the
358 HPR and consequently prevent the H_{2aq} from reaching inhibitory levels (Eq. 4). However, in
359 our study the effect on the specific HPR, BGR and GCR was simultaneous (Fig. 2), indicating
360 that H_{2aq} directly acts on all rates of dark fermentation.

361 **4.3. Hydrogen and biomass yields under different operating conditions and H_{2aq}**

362 **concentrations**

363 Despite the inhibition by H_{2aq} discussed in section 4.2, the HY remained high at 3.0 (± 0.0)
364 mol H_2 /mol glucose (Table 4) when applying 300 rpm agitation without GaR in assay 1. The
365 HY increased even further to 3.5 mol H_2 /mol glucose coupled with a decrease of the LA/AA
366 ratio (Table 4) when GaR maintained the H_{2aq} in equilibrium with the gas phase.

367 *T. neapolitana* predominately ferments glucose via the AA and the LA pathways, with the
368 former leading to hydrogen production and one additional mole of ATP [7].

369 The AA pathway is thereby energetically more challenging [1], because the formation of
370 hydrogen requires a high free Gibbs energy change as protons are poor electron acceptors
371 [39]. The reaction to gaseous hydrogen is favored by low hydrogen concentrations and high
372 temperatures as explained in detail by Verhaart et al. [39]. This indicates that the
373 temperature was most likely responsible for the high HYs at sole agitation of 300 rpm. The
374 additional decrease of H_{2aq} by GaR caused an additional energetical advantage and allowed
375 the further shift towards the AA pathway leading to the increase of the HY.

376 A similar effect on the HY was obtained by Beckers et al. [29], measuring H_{2aq} in 200 mL
377 serum bottles inoculated with *Clostridium butyricum* at 30°C. Unstirred cultures experienced
378 a supersaturation up to 7 times the equilibrium concentration resulting in a reduced HY of
379 1.16 mol H_2 /mol glucose, in comparison to 1.52 mol H_2 /mol glucose obtained when agitating
380 at 120 rpm. The inhibition by hydrogen has also been demonstrated previously in *T.*
381 *neapolitana* cultivation using closed 120 mL serum bottles. d'Ippolito et al. [12] were able to
382 increase the HY by reducing the culture/headspace ratio leading to a lower hydrogen partial
383 pressure in the gas phase.

384 When GaR was applied at high cell concentrations, a lower LA/AA ratio indicates that more
385 energy was gained by the culture per unit of substrate. Concomitantly, a higher BMY was
386 observed, which suggests that biomass production did not, as often assumed, compete with
387 the final product formation, but rather increased simultaneously when the environmental
388 conditions were optimized. The decrease of the biomass concentration at 500 rpm depicted
389 in Fig. 1C was caused by a change of *T. neapolitana* cell morphology in response to nutrient
390 limitations. This phenomenon interferes with the optical density measurement as described
391 in more detail by Dreschke et al. [34], whereas the actual biomass concentration is not
392 affected. In our study, the variation of HY and BMY was much lower than that of HPR under

393 different operating conditions, indicating that hydrogen inhibition primarily acts on the
394 process rates. We assume that a reduction of the dark fermentation rate by the culture at
395 high H_{2aq} concentrations aims to prevent the inhibition of the AA pathway which allows the
396 higher energy yield.

397 **4.4. Biogas recirculation as a strategy to prevent hydrogen supersaturation**

398 A large number of studies used headspace sparging with gases such as N_2 or CO_2 (Table 1) to
399 counteract hydrogen inhibition by lowering H_{dis} (Eq. 4). For instance, Sonnleitner et al. [26]
400 observed an increase of HPR from 25 to 119 mL/L/h when sparging the headspace of a
401 *Caldicellulosiruptor saccharolyticus* culture with N_2 at 1 L/L/h. However, while sparging with
402 external gases is generally successful to improve the process performance (Table 1), it
403 inevitably leads to an undesired dilution of the produced hydrogen and consequently an
404 increase of costs for gas purification. In contrast, the concentration of hydrogen in the
405 produced gas remains high when GaR is applied.

406 To our knowledge, only two studies have so far focused on the recirculation of the H_2 -rich
407 biogas in dark fermentation. Kim et al. [22] used GaR at flow rates ranging from 100 to 400
408 mL/min in a CSTR with a mixed culture at 35°C. They obtained similar HPRs and HYs, i.e.
409 0.77–0.86 and 0.77 mol H_2 / mol hexose, respectively, with and without GaR. This suggests
410 that at the prevalent reactor conditions, hydrogen did not supersaturate in the liquid phase
411 which rendered GaR ineffective. Bakonyi et al. [23] recirculated the internal biogas at two
412 different H_2 concentrations into a CSTR using a mixed culture at 35°C. The recirculation of
413 the less concentrated gas (50% H_2) resulted in a HPR of 8.9 – 9.2, whereas the use of a more
414 concentrated gas (66% H_2) reduced the HPR to 2.7 – 3.0 L H_2 /L/d, compared to 7.4 L H_2 /L/d
415 obtained without recirculation. Unfortunately, a direct measurement of H_{2aq} was not
416 included in any of the two studies, making the correlation of the reactor performance to H_{2aq}

417 impossible. In our study, we directly demonstrate the impact of stirring speed and GaR on
418 H_{2aq} and correlate it to the process performance. GaR has proven highly effective to provide
419 an adequate gas-liquid mass transfer, that can be readily adjusted by adapting the
420 recirculation flow to meet the requirements of the system. Furthermore, the results confirm
421 that maintaining H_{2aq} in equilibrium with the gas phase is sufficient to reach high HY up to
422 3.5 mol H_2 /mol glucose (Table 4) and a high specific HPR of 1090 ± 91 mL/h/g CDW (Table 3).

423 **Conclusions**

424 This study confirms that hydrogen supersaturates in the liquid phase and strongly inhibits
425 dark fermentation by *T. neapolitana cf. capnolactica*. GaR and the sole agitation at 500 rpm
426 efficiently reduced the H_{2aq} (i.e. 30.1 ± 4.4 mL/L) observed at low cell concentration and
427 agitation of 100 rpm to below the equilibrium value suggested by Henry's law (i.e. 9.7 mL/L).
428 At high cell concentrations (i.e. 0.79 g CDW/L), 500 rpm agitation did not provide sufficient
429 gas-liquid mass transfer to prevent H_{2aq} supersaturation, which was instead counteracted by
430 GaR. High H_{2aq} concentrations led to thermodynamic constraints and the reciprocal influence
431 of H_{2aq} and HPR, which directly hampered the dark fermentation rates. In this line, we
432 observed the specific HPR increasing by 271% when adding GaR at 300 rpm, as well as a HY
433 increase from 3.0 to 3.5 mol H_2 /mol glucose. Hence, we conclude that recirculation of H_2 -
434 rich biogas is an efficient method to prevent hydrogen supersaturation and allow high
435 production rates and yields without negatively effecting the hydrogen content of the
436 produced biogas.

437

438 **Funding:** This work was supported by the Marie Skłodowska-Curie European Joint Doctorate
439 (EJD) in Advanced Biological Waste-To-Energy Technologies (ABWET) funded by Horizon
440 2020 under grant agreement no. 643071.

441 **Acknowledgements**

442 The authors want to express their appreciation to the staff of CNR-ICB for the consistent
443 help throughout this study.

444

445

446

447

448

449

450

451

452

453

454

455

456

457

458

459

460

461

462

463

464

465 **Fig. 1:** Glucose consumption (A), cumulative hydrogen production (B) and biomass growth
466 (C) throughout the dark fermentation of 27.8 mM of glucose by *T. neapolitana cf.*
467 *capnolactica* using 300 and 500 rpm agitation speed, excluding or including recirculation of
468 the produced gas (GaR).

469
470 **Fig. 2:** Specific rates of biomass growth (BGR), glucose consumption (GCR) and hydrogen
471 production (HPR) obtained during the dark fermentation of 27.8 mM of glucose by $0.79 (\pm$
472 $0.03)$ g CDW /L of *T. neapolitana cf. capnolactica* using 300 and 500 rpm agitation speed,
473 excluding or including recirculation of the produced gas (GaR). Specific rates were calculated
474 based on the initial biomass concentration in the reactor expressed as cell dry weight (CDW).
475

476 **Fig. 3:** Hydrogen production rate (HPR) (A) and concentration of hydrogen in the liquid phase
477 (H_{2aq}) (B) at different operating conditions using 100, 200, 300 and 500 rpm as well as 200
478 rpm and 500 rpm with gas recirculation (GaR) for 2 h during the dark fermentation of 27.8
479 mM of glucose by *T. neapolitana cf. capnolactica*. (“HPR post GaR” – retention phase, i.e. 25
480 min after applying GaR; “HPR” – equilibrium phase, i.e. 90 min before the subsequent GaR;
481 “HPR GaR” – removal phase, i.e. when applying GaR for 5 min). The dashed line (----)
482 represents the H_{2aq} in equilibrium with the gas phase at 65% H_2 at 80 °C, i.e. 9.7 mL/L.
483

484 **Fig. 4:** Cumulative hydrogen production (●) and H_{2aq} evolution (□) during the dark
485 fermentation of 27.8 mM of glucose by *T. neapolitana cf. capnolactica* under different
486 operating conditions: (A) 100, 300 and 500 rpm agitation speed with 5 min of gas
487 recirculation (GaR) between each condition; (B) and (C) 100, 200 and 200 rpm + GaR. The
488 dashed line (----) represents the H_{2aq} in equilibrium with the gas phase at 65% H_2 at 80 °C, i.e.
489 9.7 mL/L.

490

491

492

493

494

495

496

497

498

499

500

501 **Table 1:** Different techniques applied to decrease the H_{2aq} and reduce its inhibition on dark
502 fermentation. A “x” was used to indicate if H_{2aq} was directly measured in the referenced
503 study or an effect on H_2 yield and production rate was observed.

504

505 **Table 2:** Operating conditions during assay 2. 100, 200, 300 and 500 represent the agitation
506 speed in rpm.

507

508 **Table 3:** Hydrogen production, biomass growth and glucose consumption rates during the
509 dark fermentation of 27.8 mM of glucose by *T. neapolitana cf. capnolactica* at 300 and 500
510 rpm, excluding or including recirculation of the produced gas (GaR). The rates and lag phase
511 were determined through data fitting with a modified Gompertz model. The adequateness
512 of the fit is illustrated by the coefficient of determination (R^2). Specific rates are calculated
513 based on the initial biomass concentration in the reactor.

514

515 **Table 4:** Hydrogen yield (HY), biomass yield (BMY) and glucose consumption obtained in a 2
516 L batch reactor inoculated with 0.79 (\pm 0.03) g CDW/L of *T. neapolitana cf. capnolactica*,
517 performing the dark fermentation of 27.8 mM of glucose at 300 and 500 rpm agitation
518 speed, in the presence or absence of recirculation of the produced gas (GaR).

519

520 **Table 5:** Composition of the digestate at the end of the fermentation of 27.8 mM of glucose
521 by *T. neapolitana cf. capnolactica* using 300 and 500 rpm agitation speed with or without the
522 recirculation of the produced gas (GaR).

523

524 References

525

- 526 [1] Balachandar G, Khanna N, Das D. Biohydrogen production from organic wastes by dark
527 fermentation. In: Biohydrogen. Elsevier; 2013, p. 103–144. doi:10.1016/B978-0-444-
528 59555-3.00006-4.
- 529 [2] Gupta N, Pal M, Sachdeva M, Yadav M, Tiwari A. Thermophilic biohydrogen production
530 for commercial application: The whole picture. Int J Energy Res 2016;40(2):127–45.
531 doi:10.1002/er.3438.
- 532 [3] Show KY, Lee DJ, Tay JH, Lin CY, Chang JS. Biohydrogen production: Current perspectives
533 and the way forward. Int J Hydrogen Energy 2012;37(20):15616–31.
534 doi:10.1016/j.ijhydene.2012.04.109.
- 535 [4] Sinha P, Pandey A. An evaluative report and challenges for fermentative biohydrogen
536 production. Int J Hydrogen Energy 2011;36(13):7460–78.
537 doi:10.1016/j.ijhydene.2011.03.077.
- 538 [5] Wang J, Wan W. Factors influencing fermentative hydrogen production: A review. Int J
539 Hydrogen Energy 2009;34(2):799–811. doi:10.1016/j.ijhydene.2008.11.015.
- 540 [6] Pawar SS, van Niel EWJ. Thermophilic biohydrogen production: how far are we? Appl
541 Microbiol Biotechnol 2013;97(18):7999–8009. doi:10.1007/s00253-013-5141-1.
- 542 [7] Pradhan N, Dipasquale L, d'Ippolito G, Panico A, Lens PNL, Esposito G et al. Hydrogen
543 production by the thermophilic bacterium *Thermotoga neapolitana*. Int J Mol Sci
544 2015;16(6):12578–600. doi:10.3390/ijms160612578.
- 545 [8] Huber R, Hannig M. Thermotogales. In: Dworkin M, Falkow S, Rosenberg E, Schleifer K-
546 H, Stackebrandt E, editors. The Prokaryotes. New York, NY: Springer New York; 2006, p.
547 899–922. doi:10.1007/0-387-30747-8_38.
- 548 [9] Cappelletti M, Bucchi G, Sousa Mendes J de, Alberini A, Fedi S, Bertin L et al.
549 Biohydrogen production from glucose, molasses and cheese whey by suspended and
550 attached cells of four hyperthermophilic *Thermotoga* strains. J Chem Technol
551 Biotechnol 2012;87(9):1291–301. doi:10.1002/jctb.3782.
- 552 [10] Dipasquale L, d'Ippolito G, Gallo C, Vella FM, Gambacorta A, Picariello G et al. Hydrogen
553 production by the thermophilic eubacterium *Thermotoga neapolitana* from storage
554 polysaccharides of the CO₂-fixing diatom *Thalassiosira weissflogii*. Int J Hydrogen Energy
555 2012;37(17):12250–7. doi:10.1016/j.ijhydene.2012.05.160.
- 556 [11] de Vrije T, Budde MA, Lips SJ, Bakker RR, Mars AE, Claassen PA. Hydrogen production
557 from carrot pulp by the extreme thermophiles *Caldicellulosiruptor saccharolyticus* and
558 *Thermotoga neapolitana*. Int J Hydrogen Energy 2010;35(24):13206–13.
559 doi:10.1016/j.ijhydene.2010.09.014.
- 560 [12] d'Ippolito G, Dipasquale L, Vella FM, Romano I, Gambacorta A, Cutignano A et al.
561 Hydrogen metabolism in the extreme thermophile *Thermotoga neapolitana*. Int J
562 Hydrogen Energy 2010;35(6):2290–5. doi:10.1016/j.ijhydene.2009.12.044.
- 563 [13] Dreschke G, Papirio S, Sisinni DMG, Lens PNL, Esposito G. Effect of feed glucose and
564 acetic acid on continuous biohydrogen production by *Thermotoga neapolitana*.
565 Bioresour Technol 2019;273:416–24. doi:10.1016/j.biortech.2018.11.040.
- 566 [14] Nguyen T-AD, Han SJ, Kim JP, Kim MS, Sim SJ. Hydrogen production of the
567 hyperthermophilic eubacterium, *Thermotoga neapolitana* under N₂ sparging condition.
568 Bioresour Technol 2010;101 Suppl 1:41. doi:10.1016/j.biortech.2009.03.041.
- 569 [15] Jayasinghearachchi HS, Sarma PM, Lal B. Biological hydrogen production by extremely
570 thermophilic novel bacterium *Thermoanaerobacter mathranii* A3N isolated from oil

- 571 producing well. Int J Hydrogen Energy 2012;37(7):5569–78.
572 doi:10.1016/j.ijhydene.2011.12.145.
- 573 [16] Kraemer JT, Bagley DM. Supersaturation of dissolved H₂ and CO₂ during fermentative
574 hydrogen production with N₂ sparging. Biotechnol Lett 2006;28(18):1485–91.
575 doi:10.1007/s10529-006-9114-7.
- 576 [17] Ljunggren M, Willquist K, Zacchi G, Van Niel EWJ. A kinetic model for quantitative
577 evaluation of the effect of hydrogen and osmolarity on hydrogen production by
578 *Caldicellulosiruptor saccharolyticus*. Biotechnol Biofuels 2011;4(1):31.
579 doi:10.1186/1754-6834-4-31.
- 580 [18] Zhang Y, Zhang F, Chen M, Chu P-N, Ding J, Zeng RJ. Hydrogen supersaturation in
581 extreme-thermophilic (70°C) mixed culture fermentation. Appl Energy 2013;109:213–9.
582 doi:10.1016/j.apenergy.2013.04.019.
- 583 [19] Kim D-H, Shin H-S, Kim S-H. Enhanced H₂ fermentation of organic waste by CO₂ sparging.
584 Int J Hydrogen Energy 2012;37(20):15563–8. doi:10.1016/j.ijhydene.2012.03.071.
- 585 [20] Lamed RJ, Lobos J. H., Su T. M. Effects of Stirring and Hydrogen on Fermentation
586 Products of *Clostridium thermocellum*. Appl Environ Microbiol 1988:1216–21.
- 587 [21] Nualsri C, Kongjan P, Reungsang A, Imai T. Effect of biogas sparging on the performance
588 of bio-hydrogen reactor over a long-term operation. PLoS ONE 2017;12(2):e0171248.
589 doi:10.1371/journal.pone.0171248.
- 590 [22] Kim D, Han S, Kim S, Shin H. Effect of gas sparging on continuous fermentative hydrogen
591 production. Int J Hydrogen Energy 2006;31(15):2158–69.
592 doi:10.1016/j.ijhydene.2006.02.012.
- 593 [23] Bakonyi P, Buitrón G, Valdez-Vazquez I, Nemestóthy N, Bélafi-Bakó K. A novel gas
594 separation integrated membrane bioreactor to evaluate the impact of self-generated
595 biogas recycling on continuous hydrogen fermentation. Appl Energy 2017;190:813–23.
596 doi:10.1016/j.apenergy.2016.12.151.
- 597 [24] Kraemer JT, Bagley DM. Optimisation and design of nitrogen-sparged fermentative
598 hydrogen production bioreactors. Int J Hydrogen Energy 2008;33(22):6558–65.
599 doi:10.1016/j.ijhydene.2008.08.033.
- 600 [25] Mandal B, Nath K, Das D. Improvement of biohydrogen production under decreased
601 partial pressure of H₂ by *Enterobacter cloacae*. Biotechnol Lett 2006;28(11):831–5.
602 doi:10.1007/s10529-006-9008-8.
- 603 [26] Sonnleitner A, Peintner C, Wukovits W, Friedl A, Schnitzhofer W. Process investigations
604 of extreme thermophilic fermentations for hydrogen production: effect of bubble
605 induction and reduced pressure. Bioresour Technol 2012;118:170–6.
606 doi:10.1016/j.biortech.2012.05.046.
- 607 [27] Zhang F, Zhang Y, Chen M, Zeng RJ. Hydrogen supersaturation in thermophilic mixed
608 culture fermentation. Int J Hydrogen Energy 2012;37(23):17809–16.
609 doi:10.1016/j.ijhydene.2012.09.019.
- 610 [28] Fritsch M, Hartmeier W, Chang J. Enhancing hydrogen production of *Clostridium*
611 *butyricum* using a column reactor with square-structured ceramic fittings. Int J
612 Hydrogen Energy 2008;33(22):6549–57. doi:10.1016/j.ijhydene.2008.07.070.
- 613 [29] Beckers L, Masset J, Hamilton C, Delvigne F, Toye D, Crine M et al. Investigation of the
614 links between mass transfer conditions, dissolved hydrogen concentration and
615 biohydrogen production by the pure strain *Clostridium butyricum* CWBI1009. Biochem
616 Eng J 2015;98:18–28. doi:10.1016/j.bej.2015.01.008.
- 617 [30] Obazu FO, Ngoma L, Gray VM. Interrelationships between bioreactor volume, effluent
618 recycle rate, temperature, pH, %H₂, hydrogen productivity and hydrogen yield with

- 619 undefined bacterial cultures. *Int J Hydrogen Energy* 2012;37(7):5579–90.
620 doi:10.1016/j.ijhydene.2012.01.001.
- 621 [31] Dreschke G, Papirio S, Lens PN, Esposito G. Influence of liquid-phase hydrogen on dark
622 fermentation by *Thermotoga neapolitana*. *Renew Energy* 2019;140:354–60.
623 doi:10.1016/j.renene.2019.02.126.
- 624 [32] Paus A, Andre G, Perrier M, Guiot SR. Liquid-to-gas mass transfer in anaerobic
625 processes: Inevitable transfer limitations of methane and hydrogen in the
626 biomethanation process. *Appl Environ Microbiol* 1990;56(6):1636–44.
- 627 [33] Pradhan N, Dipasquale L, d'Ippolito G, Panico A, Lens PN, Esposito G et al. Hydrogen and
628 lactic acid synthesis by the wild-type and a laboratory strain of the hyperthermophilic
629 bacterium *Thermotoga neapolitana* DSMZ 4359 T under capnophilic lactic fermentation
630 conditions. *Int J Hydrogen Energy* 2017;42(25):16023–30.
631 doi:10.1016/j.ijhydene.2017.05.052.
- 632 [34] Dreschke G, d'Ippolito G, Panico A, Lens PNL, Esposito G, Fontana A. Enhancement of
633 hydrogen production rate by high biomass concentrations of *Thermotoga neapolitana*.
634 *Int J Hydrogen Energy* 2018. doi:10.1016/j.ijhydene.2018.05.072.
- 635 [35] Bernfeld P. Amylases, α and β . In: Chance B, editor. Preparation and assay of enzymes.
636 San Diego, Calif.: Acad. Press; 1955, p. 149–158.
- 637 [36] Mancini G, Papirio S, Lens PN, Esposito G. Increased biogas production from wheat
638 straw by chemical pretreatments. *Renew Energy* 2018;119:608–14.
639 doi:10.1016/j.renene.2017.12.045.
- 640 [37] Bastidas-Oyanedel J-R, Mohd-Zaki Z, Zeng RJ, Bernet N, Pratt S, Steyer J-P et al. Gas
641 controlled hydrogen fermentation. *Bioresour Technol* 2012;110:503–9.
642 doi:10.1016/j.biortech.2012.01.122.
- 643 [38] Sander R. Compilation of Henry's law constants (version 4.0) for water as solvent. *Atmos*
644 *Chem Phys* 2015;15(8):4399–981. doi:10.5194/acp-15-4399-2015.
- 645 [39] Verhaart MRA, Bielen AAM, van der Oost J, Stams AJM, Kengen SWM. Hydrogen
646 production by hyperthermophilic and extremely thermophilic bacteria and archaea:
647 Mechanisms for reductant disposal. *Environ Technol* 2010;31(8-9):993–1003.
648 doi:10.1080/09593331003710244.

Table 1: Different techniques applied to decrease the H_{2aq} and reduce its inhibition on dark fermentation. A “x” was used to indicate if H_{2aq} was directly measured in the referenced study or an effect on H_2 yield and production rate was observed.

Counteracting measures	H_{2aq} measurement	Effect on yield	Effect on rate	Reference
Headspace sparging with N_2	x	x		[16–18]
Headspace sparging with CO_2		x	x	[19]
Headspace sparging with N_2/H_2 , stirring		x		[20]
Sparging with biogas (CH_4)		x	x	[21]
CO_2/N_2 and internal gas injection		x		[22]
Internal CO_2 enriched gas injection		x	x	[23]
N_2 gas injection	x	x	x	[24]
Control of reactor pressure		x		[12]
Control of reactor pressure		x	x	[25,26]
Stirring and organic loading rate	x	x	x	[27]
Bubble induction		x	x	[28]
Stirring and surface enlargement	x	x	x	[29]
Recycling of degassed effluent		x	x	[30]

Table 2: Operating conditions during assay 2. 100, 200, 300 and 500 represent the agitation speed in rpm. Grey cells represent 5 min of agitation at 500 rpm in the presence of GaR.

Time [h]	0 – 15	15 – 17		17 – 19		19 – 21		21 – 23	
Assay 2A	100	GaR	300	GaR	500	GaR	300	GaR	500
2A (duplicate)	100	GaR	500	GaR	300	GaR	500	GaR	300
Assay 2B	100		200		200 + GaR		200		200 + GaR
2B (duplicate)	100		200 + GaR		200		200 + GaR		200

GaR = recirculation of the produced biogas

Table 3: Hydrogen production, biomass growth and glucose consumption rates during the dark fermentation of 27.8 mM of glucose by *T. neapolitana cf. capnolactica* at 300 and 500 rpm, excluding or including recirculation of the produced gas (GaR). The rates and lag phase were determined through data fitting with a modified Gompertz model. The adequateness of the fit is illustrated by the coefficient of determination (R^2). Specific rates are calculated based on the initial biomass concentration in the reactor.

	Specific rate	Volumetric rate	Lag phase	R^2
Hydrogen production	[mL H ₂ /h/g CDW]	[mL H ₂ /L/h]	[h]	
300 rpm	294 ± 44	235 ± 35	2.9 ± 0.2	0.982
500 rpm	695 ± 46	535 ± 35	1.3 ± 0.1	0.991
300 rpm + GaR	1090 ± 91	850 ± 71	0.4 ± 0.0	0.994
500 rpm + GaR	1016 ± 22	813 ± 18	0.5 ± 0.1	0.991
Biomass growth	[mg CDW/h/g CDW]			
300 rpm	73 ± 11			0.981
500 rpm	266 ± 9			0.996
300 rpm + GaR	423 ± 9			0.996
500 rpm + GaR	431 ± 9			0.996
Glucose consumption	[mmol glucose/h/g CDW]			
300 rpm	4.4 ± 1.3			0.985
500 rpm	10.1 ± 0.6			0.990
300 rpm + GaR	13.3 ± 0.8			0.991
500 rpm + GaR	12.7 ± 0.2			0.985

Table 4: Hydrogen yield (HY), biomass yield (BMY) and glucose consumption obtained in a 2 L batch reactor inoculated with 0.79 (\pm 0.03) g CDW/L of *T. neapolitana cf. capnolactica*, performing the dark fermentation of 27.8 mM of glucose at 300 and 500 rpm agitation speed, in the presence or absence of recirculation of the produced gas (GaR).

Operating condition	HY [mol H ₂ /mol glucose]	BMY [g CDW/mol glucose]	Glucose consumption [%]
300 rpm	3.0 \pm 0.0	16.7	82
500 rpm	3.2 \pm 0.1	21.9	89
300 rpm + GaR	3.5 \pm 0.2	24.8	88
500 rpm + GaR	3.3 \pm 0.1	27.7	89

Table 5: Composition of the digestate at the end of the fermentation of 27.8 mM of glucose by *T. neapolitana cf. capnolactica* using 300 and 500 rpm agitation speed with or without the recirculation of the produced gas (GaR).

Operating condition	AA [mM] (yield [mol/mol glu])	LA [mM] (yield [mol/mol glu])	Alanine [mM]	Ratio LA/AA	Residual glucose [mM]	End product balance [%] ¹
300 rpm	32.3 ± 4.3 (1.4)	10.0 ± 1.0 (0.44)	1.1 ± 0.1	0.31	4.9 ± 2.7	96
500 rpm	37.7 ± 2.7 (1.5)	8.1 ± 0.2 (0.33)	1.0 ± 0.1	0.21	3.0 ± 0.4	95
300 rpm + GaR	39.2 ± 1.2 (1.6)	4.4 ± 0.1 (0.18)	0.9 ± 0.0	0.11	3.3 ± 0.2	92
500 rpm + GaR	38.7 ± 2.2 (1.6)	5.1 ± 0.5 (0.21)	0.8 ± 0.0	0.13	3.1 ± 0.4	92

¹End product balance was calculated by summing AA, LA, alanine and residual glucose and referring it to the theoretical end product formation associated with the initial glucose concentration.

Figure 1

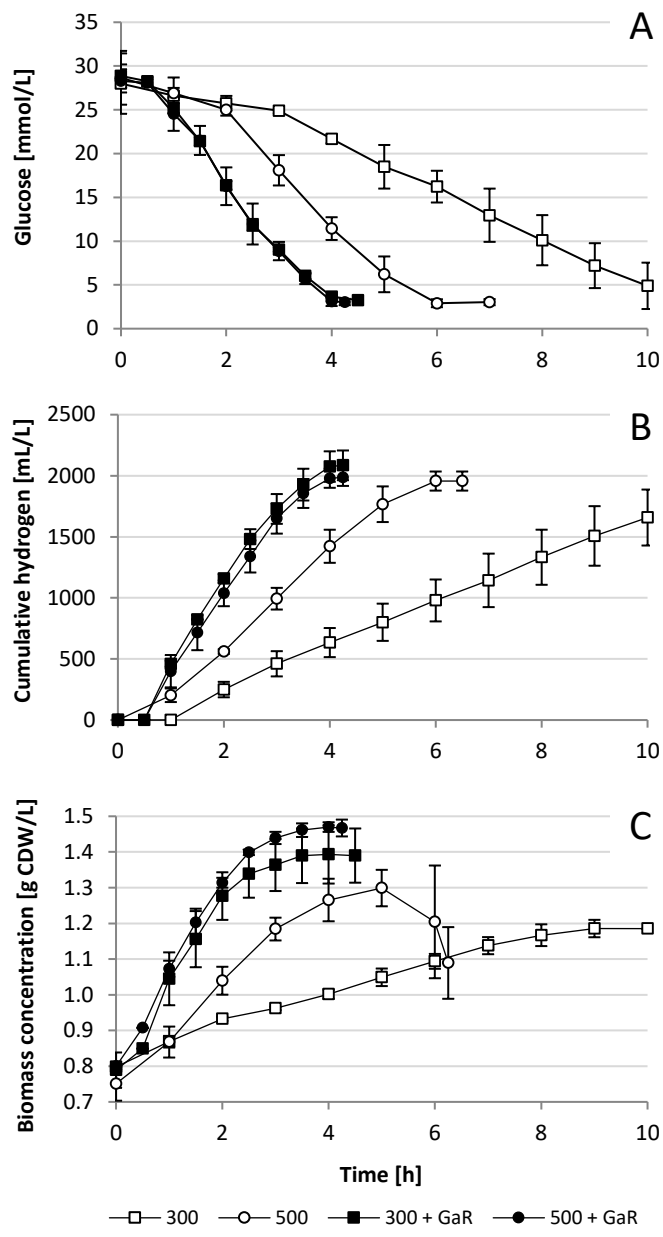


Figure 2

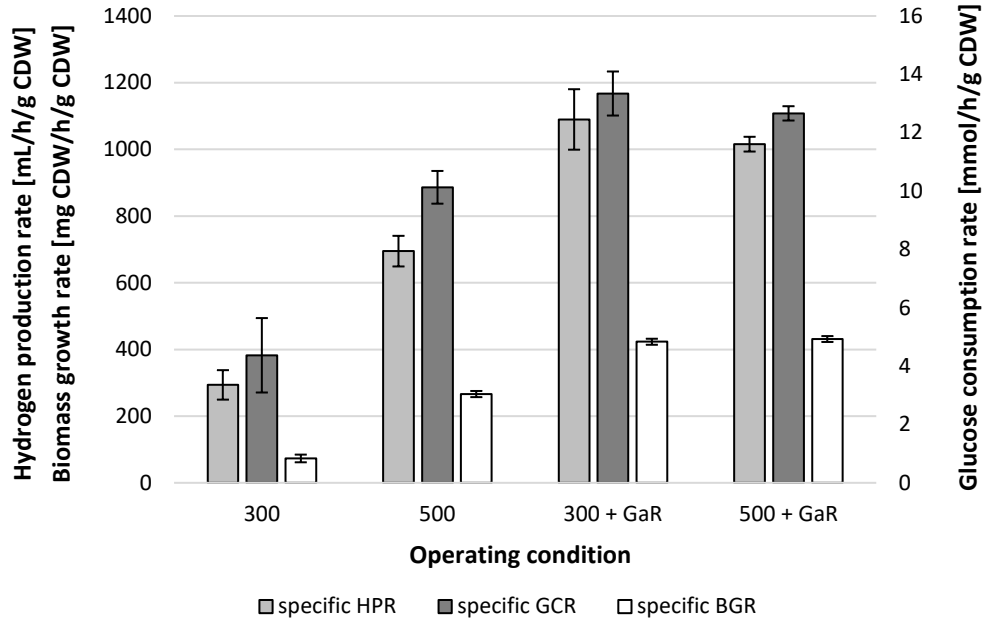


Figure 3

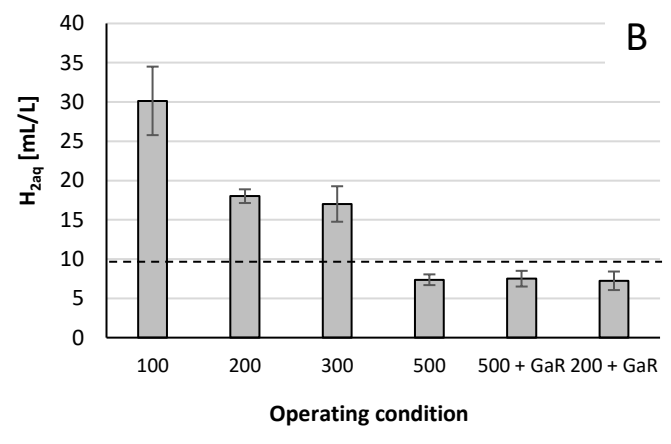
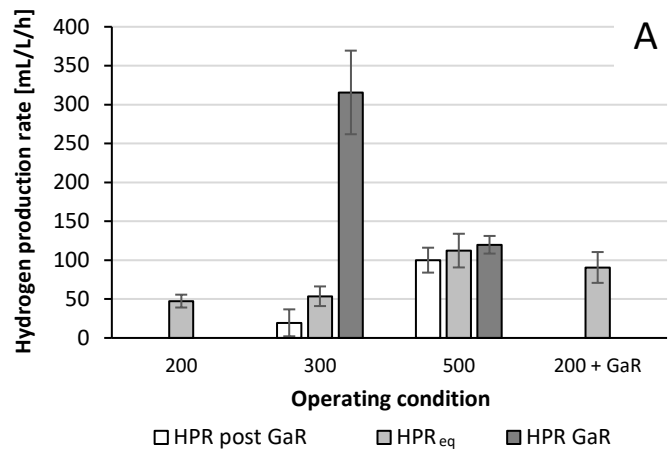
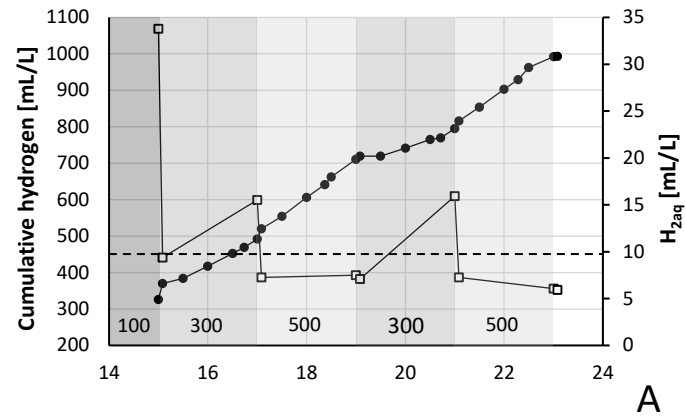
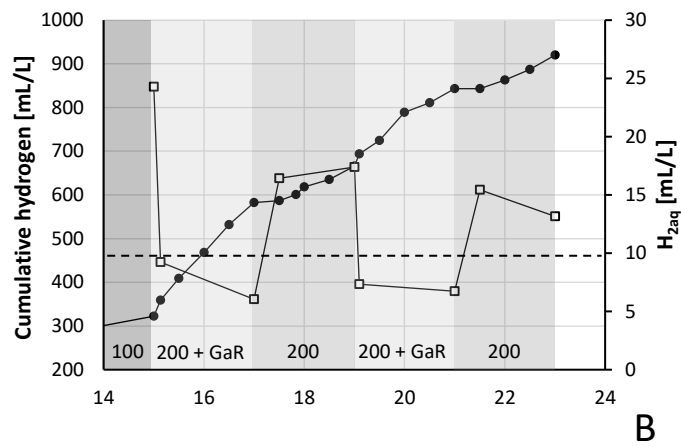


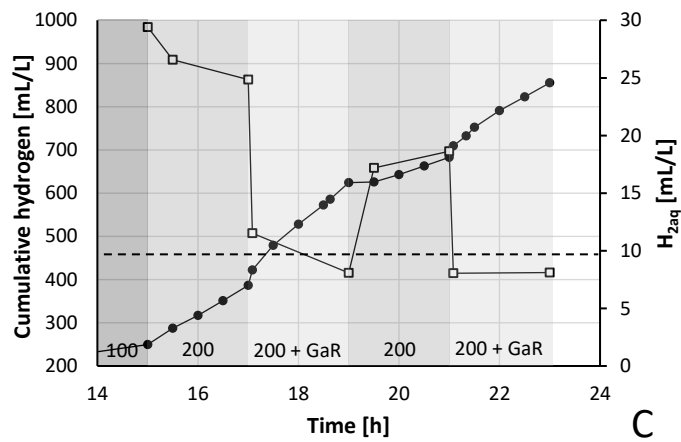
Figure 4



A



B



C